EUROPEAN CENTRAL BANK
EUROSYSTEM

Working Paper Series

Dimitris Korobilis, Bettina Landau,
Alberto Musso, Anthoulla Phella

The time-varying evolution of inflation risks

No 2600 / October 2021

Abstract

This paper develops a Bayesian quantile regression model with time-varying parameters (TVPs) for forecasting inflation risks. The proposed parametric methodology bridges the empirically established benefits of TVP regressions for forecasting inflation with the ability of quantile regression to model flexibly the whole distribution of inflation. In order to make our approach accessible and empirically relevant for forecasting, we derive an efficient Gibbs sampler by transforming the state-space form of the TVP quantile regression into an equivalent high-dimensional regression form. An application of this methodology points to a good forecasting performance of quantile regressions with TVPs augmented with specific credit and money-based indicators for the prediction of the conditional distribution of inflation in the euro area, both in the short and longer run, and specifically for tail risks.

Keywords: Quantile regression; MCMC; time-varying parameters; Bayesian shrinkage; Horseshoe; euro area; inflation tail risks.

JEL Classification: C11, C22, C52, C53, C55, E31, E37, E51

Non-Technical Summary

The prediction of inflation risks is a fundamental task of central banks whose primary objective is the maintenance of price stability. For this purpose, it is of paramount importance to develop models which allow for a useful prediction of inflation risks, that is, the risk of extreme realisations of inflation that correspond to the tails of its distribution.

This paper provides an exploration of the extent to which some modelling extensions allow for an improvement of the prediction of the distribution of inflation, concentrating on its left (negative or low inflation) and right (high inflation) tails. The analysis is carried out in the context of a time-series quantile regression setting that has proven to be particularly useful in macroeconomic forecasting (e.g., Adrian et al. (2019)). Within this econometric framework, we explore two possible enhancements to improve inflation risk forecasting: first, the role of financial indicators and, second, the role of time-varying parameters.

While the role of specific financial indicators in the prediction of inflation risks has been assessed before (e.g., López-Salido and Loria (2019)), the current analysis is the first to provide a systematic assessment of a broad set of indicators, including both financial quantities and financial prices.

The specification and estimation of time-varying parameter quantile regression (TVP-QR) models is not novel (e.g., Kim (2007), Cai and Xu (2009), and Wu and Zhou (2017)). In contrast to previous contributions, however, our proposed framework is Bayesian, meaning that error and parameter distributions are all flexible parametric rather than nonparametric. Our main methodological contribution is to propose a Markov chain Monte Carlo (MCMC) algorithm that makes estimation of, and forecasting with, the TVP-QR model feasible and fast even over a fine grid of quantiles.

We establish the benefits of our approach using both synthetic and real data. When generating synthetic data from regressions with time-varying parameters and flexible error distributions we find that our framework recovers the true parameters with higher accuracy compared to non-quantile time-varying parameter regressions that rely on a Gaussian disturbance term. Additionally, we show using these simulated data examples that our algorithm is able to track complex patterns of time-variation in parameters.

We apply this flexible framework to the problem of forecasting core consumer price inflation in the euro area using various financial indicators, both four-quarters ahead and twelve-quarters ahead. Using quarterly observations from 1990 to 2019, we find that a number of specific financial volume indicators such as loans to the private sector, loans to households and narrow money (M1) often provide the largest inflation tail risk forecasting gains, especially in the context of quantile regressions with time-varying parameters or quantile regression-based augmented Phillips curve models with time-varying parameters. A comparison of several different models and financial indicators allows to conclude that such forecast gains derive both from the predictive informational content of such specific financial volume indicators and from the benefits of modelling time-varying parameters in the context of quantile regressions.

1 Introduction

The objective of this paper is to uncover which models allow for an enhanced prediction of inflation risks, that is, the risk of extreme realisations of inflation that correspond to the tails of its distribution. For this purpose, we explore jointly two main modelling directions. First, we assess the role of financial indicators in forecasting the distribution of inflation, concentrating on its left (negative or low inflation) and right (high inflation) tails. To address this question, we adopt a time-series quantile regression setting that has proven to be particularly useful in macroeconomic forecasting. Using such setting, Adrian et al. (2019) show that the risks of low real economic activity growth are particularly sensitive to deteriorating financial conditions. Similarly, Korobilis (2017), López-Salido and Loria (2019) and Tagliabracci (2020) use quantile regressions to explore the factors that affect different quantiles of the inflation distribution. Within this econometric framework, our second research question is methodological and pertains to understanding the role of time-varying parameters in a quantile regression. Time-varying parameters (TVPs) have a long tradition in macroeconomics (see for example Cooley and Prescott, 1976) and there is a large econometric literature that also attempts to use TVP regressions to identify good predictors of the mean of inflation at different points in time (Koop and Korobilis, 2012).[1] Furthermore, Rossi (2020) points out the importance of modelling time-varying volatility for predicting densities in macroeconomic data and it has also recently been argued that regressions featuring time-varying variances can forecast output risks as well as constant parameter quantile regression models (Brownlees and Souza, 2021; Carriero et al., 2020). However, little is known about whether one can further improve forecasts by combining the benefits of time-varying parameters with the flexibility of a quantile regression setting.

Taking all the considerations above into account, our proposal is to use a time-varying parameter quantile regression (TVP-QR) model for forecasting the full distribution of inflation. At the conceptual level, specification of a TVP-QR model is not novel.[2] However, serious inference challenges are in order with the implementation of this model in a time-series forecasting context. Kim (2007), Cai and Xu (2009), and Wu and Zhou (2017) use nonparametric methods, such as splines and local polynomials, to estimate TVP-QR models. However, nonparametric estimators are not

[1] Summarising the results of a comprehensive comparison of different models, data and transformations, Faust and Wright (2013) argue that a basic principle in forecasting inflation is to allow for its local mean to be smoothly varying over time, and an obvious way of doing this is via time-varying parameters (Stock and Watson, 2007).

[2] For related Bayesian modeling approaches, see Gerlach et al. (2011), Griffin and Mitrodima (2020) and Pfarrhofer (2021).

straightforward to interpret and they are hard to apply to models with more predictors/indicators than time-series observations (as is often the case with euro area macroeconomic data) or if the interpretation of coefficients is key for policy purposes. In contrast to previous contributions, our proposed framework is Bayesian, meaning that error and parameter distributions are all flexible parametric rather than nonparametric. We approximate the quantile regression (QR) problem with an asymmetric Laplace error distribution (Kozumi and Kobayashi, 2011). The evolution of time-varying parameters follows a random walk specification which is traditionally tackled with standard Markov chain Monte Carlo (MCMC) algorithms for state-space models; see for example the Bayesian quantile state-space model of Gonçalves et al. (2020). However, in a QR setting we need to estimate separate regressions for each quantile level, making MCMC estimation cumbersome and costly for the purpose of recursive forecasting.[3] Our main methodological contribution is to propose an MCMC algorithm that makes estimation and forecasting with the TVP-QR model feasible. We borrow ideas from Korobilis (2021) and write the TVP-QR model as an equivalent high-dimensional (quantile) regression. The resulting approximation-free algorithm ends up being a minor reparameterisation of the efficient algorithm of Chan and Jeliazkov (2009), but it is computationally much faster, thereby allowing estimation of the TVP-QR model over a fine grid of quantiles.

We establish the benefits of our approach using both synthetic and real data. When generating synthetic data from regressions with time-varying parameters and flexible error distributions we find that our framework recovers the true parameters with higher accuracy compared to non-quantile TVP regressions that rely on a Gaussian disturbance term. Additionally, we show using these simulated data examples that our algorithm is able to track complex patterns of time-variation in parameters. We achieve this by adopting the *horseshoe prior for sparse signals* of Carvalho et al. (2010), which in our setting allows for shrinkage of the time-varying parameters towards few structural breaks, or even time-invariance, without any dependence on prior tuning of hyperparameters. That way, we fully address concerns in Amir-Ahmadi et al. (2020) about the impact that prior hyperparameter choice has on estimation of TVPs, making the new estimation algorithm both fast and easy to use by less experienced users.

We apply this flexible framework to the problem of forecasting core consumer price

[3] Gonçalves et al. (2020) propose a straightforward MCMC algorithm for general quantile state-space models, but they acknowledge that this algorithm is very slow when iterating over quantiles, so they end up proposing a faster, approximate algorithm. Similarly, Lim et al. (2020) estimate a TVP-QR model but estimation is based on approximate variational Bayes methods.

inflation in the euro area using various financial indicators, both in the short run (four-quarters ahead) and the medium run (twelve-quarters ahead). Using quarterly observations from 1990 to 2019, we find that a number of specific financial volume indicators such as loans to the private sector, loans to households and narrow money (M1) often provide the largest inflation tail risk forecasting gains, especially in the context of quantile regressions with time-varying parameters or quantile regression-based augmented Phillips curve models with time-varying parameters. A comparison of several different models and financial indicators, including both financial prices and financial volumes, allows to conclude that such forecast gains derive both from the predictive informational content of such specific financial volume indicators and from the benefits of modelling time-varying parameters in the context of quantile regressions.

The paper is organised as follows. The next section describes the Bayesian TVP-QR model, its prior distributions, and our efficient MCMC estimation approach. In Section 3 we conduct a small Monte Carlo experiment to establish that the TVP-QR model can recover estimates of the true TVPs much more accurately than the default TVP regression with Gaussian errors and stochastic volatility. In Section 4 we show the quantitative results from a large-scale exercise forecasting euro area core inflation involving versions of our proposed model using different indicators, as well as various competing methodologies. Section 5 concludes the paper.

2 Bayesian time-varying parameter quantile regression

Let π_t be the scalar observation of inflation in time periods $t = 1, ..., T$, and $\boldsymbol{x}_t$ a p-dimensional vector of predetermined variables that includes an intercept, lags of inflation and exogenous predictors. We want to model the full distribution of π_t by specifying the following model for each of its quantiles $\tau = \{0.05, 0.10, ..., 0.90, 0.95\}$

$$\pi_t = \mathcal{Q}_\tau \left(\pi_t | \boldsymbol{x}_t\right) + \varepsilon_t, \tag{1}$$

where $\mathcal{Q}_\tau$ denotes the conditional quantile function of the τ-th quantile of π_t. Several linear and nonlinear quantile functions have been proposed, especially in microeconometric

applications. In a time-series context, we are interested in the following function

$$\mathcal{Q}_\tau\left(\pi_t|\boldsymbol{x}_t\right) = \boldsymbol{x}_t\boldsymbol{\beta}_t(\tau), \tag{2}$$

$$\boldsymbol{\beta}_t(\tau) = \boldsymbol{\beta}_{t-1}(\tau) + \boldsymbol{v}_t, \tag{3}$$

where $\boldsymbol{v}_t \sim N_p\left(\boldsymbol{0}, \boldsymbol{V}(\tau)\right)$ is a state error with covariance matrix $\boldsymbol{V}(\tau)$. Under this specification parameters evolve as random walks. When $\boldsymbol{V}(\tau)$ is small the evolution is smooth,[4] while for larger values of $V(\tau)$ this specification can capture abrupt jumps. Therefore, the full time-varying parameter quantile regression (TVP-QR) specification in its most general form comprises Equations (1) to (3).

2.1 A reparameterised TVP-QR model

Our first building block for estimating this model is the treatment of the error. In the constant parameter case, $\beta_t(\tau) = \beta(\tau)$, Koenker and Bassett (1978) show that univariate conditional quantiles can be obtained as the solution to the following optimisation problem

$$\widehat{\beta}(\tau) = \min_{\beta(\tau)} \mathbb{E} \sum_{t=1}^{T} \rho_\tau(\varepsilon_t), \tag{4}$$

where $\rho_\tau(u) = (\tau - \mathbb{I}(u < 0))u$ is a loss function. The minimiser of Equation (4) is equivalent to maximising an asymmetric Laplace likelihood (Yu and Moyeed, 2001), that is, the case where ε_t has density given by

$$p(\varepsilon_t; \tau, \sigma) \sim \frac{\tau(1-\tau)}{\sigma(\tau)^2}\left[e^{(1-\tau)\frac{\varepsilon_t}{\sigma(\tau)^2}}\mathbb{I}(\varepsilon_t \leq 0) + e^{-\tau\frac{\varepsilon_t}{\sigma(\tau)^2}}\mathbb{I}(\varepsilon_t > 0)\right], \tag{5}$$

where $\sigma(\tau)^2$ is a scale parameter.[5] Following Kozumi and Kobayashi (2011), the asymmetric Laplace distribution can be written as a Gaussian-Exponential scale

[4] Notice that the solution $\boldsymbol{V}(\tau) = \boldsymbol{0}$ gives the constant parameter model as a special case of the TVP model.

[5] In the time-varying parameter mean regression framework it is natural to assume the presence of stochastic volatility, σ_t^2. Combined with the typical assumption of Normality in the errors, time-varying variances are able to produce more flexible, heavy-tailed unconditional distributions of inflation. The assumption of stochastic volatility in the quantile regression model, $\sigma_t(\tau)$, is computationally trivial to incorporate. However, we have found that, unlike for longer financial data (Gerlach et al., 2011), it consistently produces inferior fit and out-of-sample forecasts for euro area inflation data, given its relatively short sample size. Even when not allowing the variance parameter to fluctuate over time, in the context of quantile regression, it still takes a different value across different quantiles, meaning that we are able to capture very complex shapes of distributions.

mixture of the form

$$(\varepsilon_t|u_t, z_t) \sim \theta(\tau)z_t + \sqrt{\sigma(\tau)^2\kappa(\tau)^2 z_t(\tau)}u_t, \tag{6}$$

where $z_t(\tau) \sim Exp(\sigma^2(\tau))$ and $u_t \sim N(0,1)$, while $\theta(\tau), \kappa(\tau)^2$ are parameters defined as $\theta(\tau) = \frac{1-2\tau}{\tau(1-\tau)}$, $\kappa(\tau)^2 = \frac{2}{\tau(1-\tau)}$. If we marginalise Equation (6) over z_t we obtain Equation (5); see more details in Appendix A and Khare and Hobert (2012). Therefore, the first modelling assumption we adopt is that the error distribution in Equation (1) follows the mixture of Normals specification in Equation (6). The benefits of this assumption are immediately visible: since the likelihood is conditionally (on z_t) Gaussian, the conditional parameter posteriors will be identical to standard expressions from linear Gaussian regression models.[6]

The second building block is the way we treat time variation. We extend ideas in Korobilis (2021) and we rewrite the model in Equations (2) - (3) as a high-dimensional regression with more covariates than observations. In particular, it is easy to show that if we stack all T observations, these equations can be rewritten as

$$\mathcal{Q}_\tau(\boldsymbol{\pi}|\mathcal{X}) = \mathcal{X}\boldsymbol{\beta}^{\Delta}(\tau), \tag{11}$$

$$\boldsymbol{\beta}^{\Delta}(\tau) = \boldsymbol{v}, \tag{12}$$

[6]It is easy to visualise this; for example in the linear QR case

$$\pi_t = \boldsymbol{x}_t\boldsymbol{\beta}(\tau) + \theta(\tau)z_t + \sqrt{\sigma(\tau)^2\kappa(\tau)^2 z_t(\tau)}u_t, \tag{7}$$

if we condition on z_t (i.e. we treat it as a known parameter) we can write

$$\pi_t - \theta(\tau)z_t = \boldsymbol{x}_t\boldsymbol{\beta}(\tau) + \sigma(\tau)\kappa(\tau)\sqrt{z_t(\tau)}u_t, \Rightarrow \tag{8}$$

$$\frac{\pi_t - \theta(\tau)z_t}{\kappa(\tau)\sqrt{z_t}} = \left(\frac{\boldsymbol{x}_t}{\kappa(\tau)\sqrt{z_t}}\right)\boldsymbol{\beta}(\tau) + \sigma(\tau)u_t, \tag{9}$$

$$\widetilde{\pi}_t = \widetilde{\boldsymbol{x}}_t\boldsymbol{\beta}(\tau) + \widetilde{\varepsilon}_t, \tag{10}$$

which is a linear, Gaussian regression on the data $\widetilde{\pi}_t$ and $\widetilde{\boldsymbol{x}}_t$, and the error $\widetilde{\varepsilon}_t \sim N(0, \sigma(\tau))$. Therefore, it is fairly trivial to derive conditional posteriors for $\boldsymbol{\beta}(\tau)$ and $\sigma(\tau)$ using this form.

where $\boldsymbol{\pi} = [\pi_1, ..., \pi_T]'$, $\boldsymbol{v} = [\boldsymbol{v}_1', ..., \boldsymbol{v}_T']'$ and

$$\underset{T \times Tp}{\mathcal{X} = \begin{bmatrix} x_1 & 0 & ... & 0 & 0 \\ x_2 & x_2 & ... & 0 & 0 \\ ... & ... & ... & ... & ... \\ x_{T-1} & x_{T-1} & ... & x_{T-1} & 0 \\ x_T & x_T & ... & x_{T-1} & x_T \end{bmatrix}}, \quad \text{and} \quad \underset{Tp \times 1}{\boldsymbol{\beta}^{\Delta}(\tau) = \begin{bmatrix} \boldsymbol{\beta}_1(\tau) \\ \Delta\boldsymbol{\beta}_2(\tau) \\ ... \\ \Delta\boldsymbol{\beta}_{T-1}(\tau) \\ \Delta\boldsymbol{\beta}_T(\tau) \end{bmatrix}}. \tag{13}$$

We provide detailed derivations and discussion of this form in Appendix A. In this new formulation, all Tp coefficients of the TVP regression are stacked in a single vector, while at the same time they appear in first differences form. Specifically, in this hierarchical (multilevel) regression specification, Equation (12) can be interpreted as a prior for $\boldsymbol{\beta}_{\Delta}(\tau)$ which means that equation Equation (11) can be treated as a linear regression model and estimated using algorithms for constant parameter models. Interpretation of this formulation is straightforward as we can recover the original vector of TVPs, $\boldsymbol{\beta} = [\boldsymbol{\beta}_1(\tau)', ..., \boldsymbol{\beta}_T(\tau)']'$ as the cumulative sum of the vector of first differences, $\boldsymbol{\beta}^{\Delta}(\tau)$.

2.2 Likelihood, priors and a new Gibbs sampler

Putting together these pieces, the new parameterisation now combines Equation (1) with the distributional assumptions on the error term in Equation (6) with the reparameterised TVP function in Equations (11) and (12). The core of the TVP-QR model now has the following form

$$\boldsymbol{\pi} \quad = \quad \mathcal{X}\boldsymbol{\beta}^{\Delta}(\tau) + \theta(\tau)\boldsymbol{z}(\tau) + \widetilde{\boldsymbol{S}}\boldsymbol{u}, \tag{14}$$

where $\widetilde{\boldsymbol{S}}$ is a $T \times T$ diagonal matrix with t-th diagonal element $\sqrt{\sigma(\tau)^2\kappa(\tau)^2 z_t(\tau)}$. This model is completed by considering priors on various parameters. By definition, $z(\tau) \sim Exponential(\sigma(\tau)^2)$. The scale parameter can take the standard inverse Gamma prior, that is, $\sigma(\tau) \sim inv - Gamma(\rho_1, \rho_2)$. Finally, from Equation (12) we already discussed that $\boldsymbol{\beta}^{\Delta}(\tau)$ has a Normal prior of the form $\boldsymbol{\beta}^{\Delta}(\tau) \sim N(0, V(\tau))$. Multiplication of these priors with the reparameterised likelihood implied by the model in Equation (14), gives

the following conditional posteriors

$$\beta^{\Delta}(\tau)|\bullet \sim N\left(\boldsymbol{Q}\times\left(\mathcal{X}'\boldsymbol{U}^{-1}\widetilde{\boldsymbol{y}}\right),\boldsymbol{Q}\right), \tag{15}$$

$$\sigma(\tau)^2|\bullet \sim inv-Gamma\left(\rho_1+\frac{3T}{2},\rho_2+\sum_{t=1}^{T}\frac{(y_t^{\star})^2}{2z_t(\tau)\kappa(\tau)^2}+\sum_{t=1}^{T}z_t(\tau)\right), \tag{16}$$

$$z_t(\tau)|\bullet \sim IG\left(\frac{\sqrt{\theta(\tau)^2+2\kappa(\tau)^2}}{|y_t-\mathcal{X}_t\boldsymbol{\beta}^{\Delta}(\tau)|},\frac{\theta(\tau)^2+2\kappa(\tau)^2}{\sigma(\tau)^2\kappa(\tau)^2}\right), \tag{17}$$

where the notation $|\bullet$ means "conditioning on other parameters and data", $\boldsymbol{Q} = (\mathcal{X}'\boldsymbol{U}^{-1}\mathcal{X}+V(\tau)^{-1})^{-1}$, $\boldsymbol{U} = (\sigma(\tau)^2\kappa(\tau)^2)\times diag\left(z_1(\tau),...,z_T(\tau)\right)$, $\widetilde{\boldsymbol{y}} = (\boldsymbol{y}-\theta(\tau)\boldsymbol{z}(\tau))$, $y_t^{\star} = \left(y_t-\mathcal{X}_t\boldsymbol{\beta}^{\Delta}(\tau)-\theta(\tau)z_t(\tau)\right)$. This Gibbs sampler is a reparameterised version of the ergodic Gibbs sampler for constant parameter quantile regressions developed by Khare and Hobert (2012). Sampling from the conditional distributions is straightforward and computation can be sped up by sampling for all values of τ simultaneously, instead of sampling iteratively for each τ. The only computational challenge is sampling of the Tp elements in $\boldsymbol{\beta}^{\Delta}(\tau)$, since Tp can be very large. Bhattacharya et al. (2016) provide a very efficient way of sampling from such high-dimensional Normal posteriors, and we refer the reader to this paper and Appendix A for more information about implementation.

The reparameterised form of the TVP regression shows that this is a model with more predictors than observations (measurement matrix $\mathcal{X}$ has Tp covariates but only T observations). Therefore, it is evident that prior selection for the high-dimensional vector $\boldsymbol{\beta}^{\Delta}(\tau)$ must be done carefully; see Amir-Ahmadi et al. (2020) for a discussion of this issue. Consequently, the horseshoe prior of Carvalho et al. (2010) is adopted, due to the fact that it is shown to have excellent theoretical guarantees, thus, making it an established estimator in statistics.[7] The horseshoe prior for $\boldsymbol{\beta}^{\Delta}(\tau)$ is defined as

$$\boldsymbol{\beta}^{\Delta}(\tau)|\lambda(\tau)^2,\{\psi_i(\tau)^2\}_{i=1}^{Tp} \sim N(0,V(\tau)), \tag{18}$$

$$V_{i,i}(\tau) = \lambda(\tau)^2\psi_i(\tau)^2, \quad i=1,...,Tp,$$

$$\lambda(\tau) \sim Cauchy^{+}(0,1), \tag{19}$$

$$\psi_i(\tau) \sim Cauchy^{+}(0,1), \quad i=1,...,Tp, \tag{20}$$

[7] In linear Gaussian regression settings, the horseshoe prior is minimax in l_2 norm (van der Pas et al., 2014), attains risk equal to the Bayes oracle (Ghosh et al., 2016) and posterior credible intervals under the horseshoe prior also have good frequentist coverage properties in an asymptotic sense. More recently, Bhadra et al. (2020) show that horseshoe regularisation retains its excellent properties in several classes of complex models, including non-linear, non-Gaussian regression, and deep neural networks.

where $Cauchy^{+}$ denotes the half-Cauchy distribution on the positive reals.[8] In line with Amir-Ahmadi et al. (2020), $V(\tau)$ comprises hyperparameters that have their own prior distributions and are, thus, updated by information in the data. The fact that the hyperpriors for $\lambda(\tau)$ and $\psi_i(\tau)$ do not depend on further parameters that require tuning/calibration, makes the horseshoe a fully automatic prior that adapts equally well to low-dimensional as well as high-dimensional problems.

2.3 Noncrossing quantiles

Quantiles of a distribution have the property that they are monotonically increasing on the quantile level τ, for instance, the forecasted value of inflation at $\tau = 0.05$ should always be smaller than the value of inflation at $\tau = 0.10$. However, quantile regression models are typically estimated independently for each quantile level τ, which is also what our proposed Gibbs sampler is doing. Therefore, when estimating a quantile function without reference to other quantiles, there is no guarantee that the monotonicity assumption will always hold. To solve this issue, there are numerous ways of post-processing quantile estimates in order to ensure that estimates $\widehat{\mathcal{Q}}_{\tau_1}(y_t|x_t) > \widehat{\mathcal{Q}}_{\tau_2}(y_t|x_t)$ for $\tau_1 < \tau_2$ are not allowed.

For that reason we use the recently proposed algorithm of Rodrigues and Fan (2017) which is specifically tailored to Bayesian quantile regression using output from an MCMC algorithm (i.e. samples from the parameter posterior). This algorithm involves using a consistent MCMC-based estimator to obtain quantile regression estimates and subsequently fitting a Gaussian process regression to smooth out the quantile estimates. A key working assumption of this smoothing procedure is the combination of quantile

[8] The formulation using the half-Cauchy priors is not ideal as it does not allow straightforward derivation of conditional posteriors. Makalic and Schmidt (2016) note that the half-Cauchy distribution can be written as a mixture of inverse Gamma distributions. Therefore, the horseshoe prior can be written equivalently as

$$\begin{aligned}
\boldsymbol{\beta}^{\Delta}(\tau)|\lambda(\tau)^2, \{\psi_i(\tau)^2\}_{i=1}^{Tp} &\sim N(0, V(\tau)), && (21)\\
V_{i,i}(\tau) &= \lambda(\tau)^2\psi_i(\tau)^2, \quad i = 1, ..., Tp, &&\\
\lambda(\tau)^2|\xi(\tau) &\sim inv-Gamma\left(1/2, 1/\xi(\tau)\right), && (22)\\
\xi(\tau) &\sim inv-Gamma\left(1/2, 1\right), && (23)\\
\psi_i(\tau)^2|\zeta_i(\tau) &\sim inv-Gamma\left(1/2, 1/\zeta_i(\tau)\right), && (24)\\
\zeta_i(\tau) &\sim inv-Gamma\left(1/2, 1\right), && (25)
\end{aligned}$$

which is a formulation that allows for straightforward calculation of conditional posteriors; see Makalic and Schmidt (2016) for more details on posterior computation. It is trivial to show that one can simply add the formulas for the conditional posteriors of $\lambda(\tau)^2, \xi, \psi_i(\tau)^2, \zeta_i(\tau)$ to the Gibbs sampler in Equations (15)-(17).

function estimates $\widehat{\mathcal{Q}}_\tau(y_t|x_t)$ (which are obtained from estimation of the TVP-QR) with the information that neighboring quantiles $\tau^\star \neq \tau$ convey for the quantile function of τ. Based on results for the asymmetric Laplace distribution, Rodrigues and Fan (2017) show that one can use the following auxiliary model to obtain information from neighboring quantiles:

$$\mathcal{Q}_{\tau,\tau^\star}(y_t|x_t) = \begin{cases} x_t\beta(\tau^\star) + \frac{\sigma(\tau^\star)}{1-\tau^\star}\log\left(\frac{\tau}{\tau^\star}\right), & if \quad 0 \leq \tau \leq \tau^\star, \\ \\ x_t\beta(\tau^\star) - \frac{\sigma(\tau^\star)}{\tau^\star}\log\left(\frac{1-\tau}{1-\tau^\star}\right), & if \quad \tau^\star \leq \tau \leq 1, \end{cases} \tag{26}$$

where $\mathcal{Q}_{\tau,\tau^\star}(y_t|x_t)$ is the induced quantile, and $\tau, \tau^\star \in \{0.05, 0.10, ..., 0.90, 0.95\}$. When $\tau = \tau^\star$ then $\mathcal{Q}_{\tau,\tau^\star}(y_t|x_t) \equiv \mathcal{Q}_\tau(y_t|x_t)$, that is, the induced quantile is equivalent to the estimated quantile based on our model. However, for all other levels of $\tau^\star$ we obtain additional induced quantile values that provide information for the quantile curve at τ. The principle is that the closer $\tau^\star$ is to τ, the more information its quantile curve can provide for estimation of the quantile curve at τ.

Given that there are 19 values in the set $\tau, \tau^\star \in \{0.05, 0.10, ..., 0.90, 0.95\}$, in our application $\mathcal{Q}_{\tau,\tau^\star}(y_t|x_t)$ is a 19×19 matrix. The diagonal elements of this matrix are identical to $\mathcal{Q}_\tau(y_t|x_t)$ (after we have estimated our model, they are identical to $\widehat{\mathcal{Q}}_\tau(y_t|x_t)$). Rodrigues and Fan (2017) specify a Gaussian process regression that ends up being equivalent to a weighting scheme where for each τ the quantiles $\mathcal{Q}_{\tau,\tau^\star}(y_t|x_t)$ take increasingly more weight the closer $\tau^\star$ is to τ. That way, the induced quantile at $\tau = \tau^\star$ (i.e. $\mathcal{Q}_\tau(y_t|x_t)$) takes the most weight and very distant quantiles get decreasing weights. It is very trivial to specify and implement this weighting/smoothing scheme, and we refer the reader to Rodrigues and Fan (2017) for more details.[9] Proposition 2 in that paper shows that this smoothed estimate of the quantiles is consistent, and it is guaranteed to provide a non-crossing solution.

[9]Their algorithm introduces two new parameters, σ^2_κ and b (using their notation). We follow the authors and set $\sigma^2_\kappa = 100$ and we select the minimum b that provides a non-crossing solution.

3 Simulation study

In this section we use artificial data in order to examine the performance of our proposed algorithm. We generate data from the following time-varying regression model

$$y_t = x_t\beta_t + \varepsilon_t, \tag{27}$$

$$\beta_t = \mu + 0.99(\beta_{t-1} - \mu) + T^{-\frac{1}{2}}u_t, \tag{28}$$

where $x \sim N(0, I_2)$ is a vector of $p = 2$ synthetic predictors, $\mu \sim U(-2, 2)$ is the long-run mean of β_t[10], and $u_t \sim N(0, I)$. Since in the empirical section we are interested in capturing predictors that are short-lived, we artificially shrink all values of $\beta_{1,t}$ to be zero for $t > T/3$, that is, the first predictor is only relevant for y only for the first third of the sample. The second predictor in the vector x is left unrestricted (i.e. not zero) in all periods.

Regarding the distribution of ε_t, we follow the Monte Carlo design in Yu (2017), and consider eight different choices:

1. Gaussian: $N(0, 1^2)$
2. Skewed : $1/5N(-22/25, 1^2) + 1/5N(-49/125, (3/2)^2) + 3/5N(49/250, (5/9)^2)$
3. Kurtotic: $2/3N(0, 1^2) + 1/3N(0, (1/10)^2)$
4. Outlier : $1/10N(0, 1^2) + 9/10N(0, (1/10)^2)$
5. Bimodal : $1/2N(-1, (2/3)^2) + 1/2N(1, (2/3)^2)$
6. Bimodal, separate modes: $1/2N(-3/2, (1/2)^2) + 1/2N(3/2, (1/2)^2)$
7. Skewed bimodal: $3/4N(-43/100, 1^2) + 1/4N(107/100, (1/3)^2)$
8. Trimodal: $9/20N(-6/5, (3/5)^2) + 9/20N(6/5, (3/5)^2) + 1/10N(0, (1/4)^2)$

This list covers a wide variety of flexible distributions, even though it is far from exhaustive.

We generate $M = 500$ datasets of length $T = 200$ from the eight time-varying parameter regression data generating processes (DGPs). For each dataset we fit two

[10]Notice that even though β_t will be estimated using the random walk evolution outlined in the previous section, in the DGP we generate its path from a persistent yet stationary process. This choice ensures that we generate time-varying parameters that are not explosive and won't cause numerical problems during estimation.

models, a "mean" TVP regression with stochastic volatility, and our quantile TVP regression. The former model is simply a special case of the latter, where we allow the variance to be time-varying, and we convert the asymmetric Laplace distribution into a Normal distribution.[11] In both cases of these two estimated models we use the same automatically tuned horseshoe prior, such that we do not influence subjectively posterior estimates of time-varying parameters, and the same efficient sampler for TVPs outlined in the previous section. Therefore, both TVP models are almost identical with the exception of the assumption about the error distribution.

With this Monte Carlo-based exercise, we aim to find out how well the asymmetric Laplace distribution can capture all of the eight error distributions we assume generated the data. In particular, we want to find out how large is the estimation error of the TVPs under the two estimated models in each of the eight DGPs, as accuracy of estimates of the TVPs will have an immediate impact on forecasting the synthetic outcome variable y_t (and, as a result, inflation π_t, when we input real data). On that account, we measure estimation accuracy using the following mean squared deviation (MSD) measure:

$$MSD_j = \frac{1}{M}\sum_{m=1}^{M}\left\{\frac{1}{T}\sum_{t=1}^{T}\left[\frac{1}{2}\sum_{i=1}^{2}\left(\beta_{t,i}^{(m)} - \widehat{\beta}_{t,i}^{(m),j}\right)^2\right]\right\}, \tag{29}$$

where $j = \{mean\ TVP\ regression,\ quantile\ TVP\ regression\}$ and $\widehat{\beta}_{t,i}^{(m),j}$ is the posterior mean of the m-th Monte Carlo iteration, of coefficient $\beta_{t,i}$, in model j. For this loss function, lower values imply lower estimation error.

Results of this exercise are presented in Table 1. Numerical entries in this table are the MSDs for the mean regression (first row) and quantile regression for quantiles $\tau = 0.05, 0.10, 0.25, 0.50, 0.75, 0.90, 0.95$ (rows 2-8). There are eight columns in this table that are associated with each of the error distributions assumed in the DGP. We observe that when the data are generated from a TVP regression with Normal errors, then the mean TVP regression estimator is optimal as it is based on the assumption that the disturbance term is Normal. In this case the quantile TVP regression is overparameterised and the asymmetric Laplace distribution assumption does not perform well. However, once we drop the assumption of Normality in the DGP, the mean regression model is performing worse than the quantile regression model in terms of estimation error. In the case of more complex distributions (Skewed bimodal, trimodal) the error produced by the mean regression model can be substantially larger.

[11] Using the scale mixtures of Normals representation in (6), we can obtain the Normal distribution by fixing $z_t(\tau) = \frac{1}{\kappa(\tau)^2} = \frac{\tau(1-\tau)}{2}$ for all t and setting $\tau = 0.5$.

Table 1: Mean squared deviations (MSDs) of estimated vs true time-varying parameters, using mean and quantile regressions

	Gaussian	Skewed	Kurtotic	Outlier	Bimodal	Bimodal sep. modes	Bimodal skewed	Trimodal
				MSD Regression				
mean	0.01	0.25	0.04	0.01	0.10	0.21	0.45	1.03
				MSD Quantile Regression				
$\tau = 0.05$	0.06	0.05	0.05	0.02	0.09	0.13	0.05	0.09
$\tau = 0.10$	0.05	0.05	0.05	0.02	0.09	0.13	0.04	0.08
$\tau = 0.25$	0.05	0.04	0.04	0.01	0.08	0.12	0.04	0.08
$\tau = 0.50$	0.05	0.04	0.04	0.01	0.06	0.11	0.03	0.06
$\tau = 0.75$	0.04	0.04	0.04	0.01	0.07	0.12	0.03	0.07
$\tau = 0.90$	0.05	0.05	0.05	0.02	0.08	0.13	0.03	0.08
$\tau = 0.95$	0.05	0.05	0.05	0.01	0.09	0.13	0.03	0.08

Notes: The mean regression model is a TVP regression with stochastic volatility assuming Normal measurement error distribution. The quantile regression model allows for time-varying coefficients of predictors and constant intercept and variance in each quantile.

In order to assist our understanding of how severe the estimation error is in the TVP regression with stochastic volatility and Normality, Figure 1 plots parameter estimates from the mean and quantile regression models in the case of the true error distribution being trimodal (eighth case). The left-hand side panel shows estimates of the coefficient on the first predictor ($\beta_{t,1}$), and the right-hand side panel estimates on the coefficient of the second predictor ($\beta_{t,2}$). In all plots the black, dotted line shows the (average over 500 iterations) true generated time-varying coefficient. The green line is the average over 500 iterations of the posterior median of the TVPs and the shaded areas are the 68% probability bands. Looking at $\beta_{t,1}$ in the left-hand side panel of the figure, the mean regression model (top graph) produces some error, as the true value of the coefficient (black dotted line) is not close to the posterior median (green line), i.e. it is not always inside the grey shaded area. In a few periods the true value of this coefficient is even outside the 68% bands. This is not the case for the quantile regression estimates for $\tau = 0.05, 0.10, 0.90, 0.95$ (bottom four graphs), where the posterior median is much closer to the true value of this coefficient. The picture of large estimation errors in the TVPs are more pronounced when we look at $\beta_{t,2}$. The "mean" regression estimates completely miss the true path of this coefficient that is used to generate the data. By contrast, the estimates of this time-varying parameter from the quantile regression are much more accurate. This graphical illustration gives an example of how the MSDs of the previous

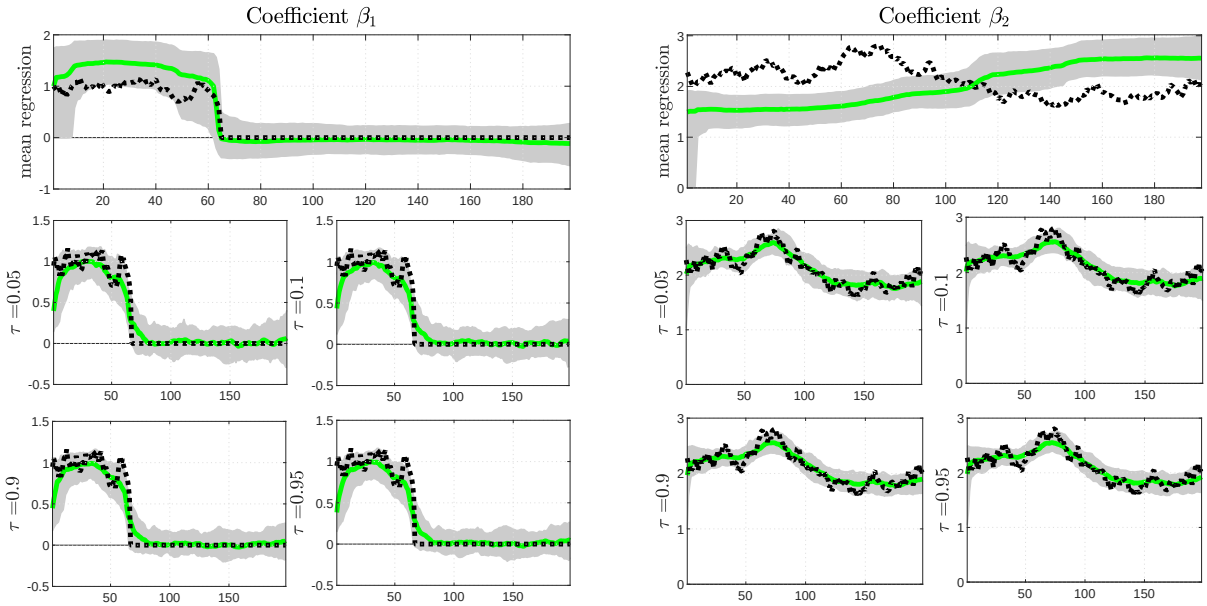

Figure 1: *Posterior estimates of time-varying parameters (TVPs) estimated using mean (upper panels) and quantile (middle and bottom panels) regressions. The five panels on the left pertain to coefficient β_{1t} in our DGP, and the five panels on the right to coefficient β_{2t}. The DGP used to produce this figure is that of a time-varying regression model with a trimodal error distribution. Mean regression is done under the standard assumption of a Normal error distribution, while the quantile regression is estimated using the flexible asymmetric Laplace distribution. Black lines are the true TVPs, which are the same for both the mean and quantile regressions. The green lines are the averages (over 500 Monte Carlo iterations) of the estimated posterior means, and the shaded areas are the 68 percent probability bands.*

table translate into significant estimation errors. Consequently, when our data distribution is non-Gaussian (which is the case with inflation and several other macroeconomic and financial variables), then our proposed TVP-QR methodology will dominate traditional TVP regressions with stochastic volatility.

4 Forecasting inflation risks in the euro area

4.1 Data

In order to assess the practical usefulness of the proposed approach for the projection of the conditional distribution of inflation, we concentrate on euro area HICP excluding energy and food inflation (henceforth referred to as core HICP inflation) developments from the first quarter of 1990 to the fourth quarter of 2019 (see Figures B1 and B2 in Appendix B). Taking core inflation instead of headline (total) HICP inflation as reference allows abstracting from the influence of temporary factors such as oil price and exchange

rate swings and focusing on more fundamental forces driving inflation tail risks. For core HICP quarterly inflation (measured by the annualised quarter-on-quarter growth rate of HICP excluding energy and food) over the whole sample size (1990Q1-2019Q4) the 5th and 95th percentiles correspond to quarterly inflation rates at 0.7 percent and 4.2 percent, respectively (see Table B2 in Appendix B). The unconditional distribution of core HICP quarterly inflation is slightly skewed to the left and exhibits a heavy right-hand side tail.

Nineteen financial indicators are considered in the analysis, including both financial volumes and financial prices. Specifically, these include four money volume indicators (M1 and M3, each expressed in annualised quarterly growth rates and as a ratio to GDP), eight credit volume indicators (total credit to the non-financial private sector, bank lending to the non-financial private sector, bank lending to non-financial corporations and bank lending to households, each expressed in annualised quarterly growth rates and as ratio to GDP), four credit spreads (for the 10-year government bond yields, lending rates to non-financial corporations, lending rates to households and investment grade corporate bond yields, all as deviations from the 3-month Euribor rate) and three additional financial indicators (stock prices, house prices and the composite indicator of systemic stress). Table B1 in Appendix B reports the details of these data and Figures B3 - B8 provide a graphical representation of them.

4.2 Models and forecast setup

The forecast performance of several models for the prediction of the conditional distribution of core HICP inflation in the short and medium term (i.e. four-quarters and twelve-quarters ahead, respectively) is assessed. The performance of various categories of models is analysed, including regression and Phillips-curve based models augmented with financial indicators, which are compared to the forecasting ability of various regression and Phillips curve models without financial predictors. For each model we entertain various specifications, ranging from quantile regressions to mean regressions, with or without time-varying parameters and with or without stochastic volatility.

We consider forecasts from the TVP-QR and numerous competitors, all of which can

be written as special cases of the general formulation[12]

$$\pi_{t+h} = c_t(\tau) + \phi_{1t}(\tau)\pi_t + \phi_{2t}(\tau)\pi_{t-1} + \beta_t(\tau)\boldsymbol{x}_t + \varepsilon_{t+h}, \quad \varepsilon_{t+h} \sim ALD(\sigma_t(\tau)), \tag{30}$$

where all the time-varying parameters follow the standard random walk assumption we established in Section 2 (but which we omit here for the sake of brevity). When $\beta_t(\tau) = 0$ the exogenous predictors $\boldsymbol{x}_t$ are absent, and we have the class of AR(2) models. When also $\phi_{1t}(\tau) = \phi_{2t}(\tau) = 0$ no lags of inflation are present and the model belongs to the class of time-varying intercept (local level) models. The assumption that ε_{t+h} follows the asymmetric Laplace distribution (ALD), coupled with the additional assumption that $\sigma_t(\tau) = \sigma(\tau)$ (see footnote 5), provides us with our proposed class of TVP quantile regression models. We already argued in footnote 11 that, when using the scale mixture of Normals representation of the ALD, we can obtain traditional TVP regression with stochastic volatility as a special case, and this result also holds for Equation (31). Finally, we can obtain constant parameter regressions and quantile regressions simply by fixing time-varying parameters to be constant over time (e.g. by setting the state variance in Equation (3) to zero). Therefore, we see that by placing appropriate restrictions in the specification above we can nest a wide class of popular forecasting models for inflation. These range from the TVP-QR, as the most flexible specification we can obtain from that equation, to the simple AR(2) model, being the most parsimonious special case. In particular, we consider forecasts from the following models

1. AR(2) model with constant parameters and variance (AR(2)) – this model is our benchmark upon which we measure the performance of all other models
2. AR(2) model with TVPs and stochastic volatility (TVP-AR-SV)
3. Time-varying intercept only model with stochastic volatility[13] (TVI-SV)
4. Quantile AR(2) with time-varying parameters (TVP-QAR)
5. Quantile regression model with time-varying intercept (TVI-QR)

[12] We specify a direct multi-step ahead forecasting model which, under the assumption that inflation is $AR(p)$, implies that the forecast errors are correlated having an $MA(h-1)$ structure. This fact suggests that in mean regression models an unbiased estimator can be made more efficient by acknowledging the effect of autocorrelated errors in the estimator variances. The parametric TVP-QR allows to easily incorporate an MA structure in the errors, and even allow for stochastic volatility if desired; see Chan (2013). Despite the fact that such an extension can be incorporated in our model, it unnecessarily increases computation. This is because we only work with the posterior mean of each TVP in each quantile level we estimate, and the variance is not used to construct predictive densities.

[13] This model is similar to the unobserved components stochastic volatility (UCSV) model of Stock and Watson (2007), although it does not assume stochastic volatility in the equation for trend inflation.

6. Mean regressions with constant parameters, exogenous predictors, and stochastic volatility (AR-SV-X)

7. Mean regressions with time-varying parameters, exogenous predictors, and stochastic volatility (TVP-AR-SV-X)

8. Quantile AR(2) with constant parameters augmented with exogenous predictors (QAR-X), and

9. Quantile AR(2) with time-varying parameters augmented with exogenous predictors (TVP-QAR-X)

On top of these purely time-series models, we also consider a semi-structural Phillips Curve (PC) formulation of Equation (30), similar to López-Salido and Loria (2019). In its most general form, the PC formulation is

$$\pi_{t+h} = (1 - \lambda_t(\tau))\pi_t^* + \lambda_t(\tau)\pi_t^{LTE} + \theta_t(\tau)\left(y_t - y_t^*\right) + \gamma_t(\tau)\pi_t^I + \beta_t(\tau)\boldsymbol{x}_t + \varepsilon_{t+h}, \quad (31)$$

where π_t^* is lagged inflation (computed as the average over the previous four quarters), π_{t+h}^{LTE} are the long-term inflation expectations (measured using Consensus 6 to 10 years ahead inflation expectations), $(y_t - y_t^*)$ is the output gap (calculated as the principal component of available estimates), and π_{t+h}^I are relative import prices (measured as the spread between import deflator inflation and core inflation). Accordingly, we consider the following specifications based on the PC restrictions:

1. Mean PC regression with stochastic volatility, no additional predictors (PC-SV)

2. Mean PC regression with time-varying parameters and stochastic volatility, no additional predictors (TVP-PC-SV)

3. Quantile PC regression, no additional predictors (QPC)

4. Quantile PC regression with time-varying parameters, no additional predictors (TVP-QPC)

5. Mean PC regression with stochastic volatility, with additional predictors (PC-SV-X)

6. Mean PC regression with time-varying parameters and stochastic volatility, with additional predictors (TVP-PC-SV-X)

7. Quantile PC regression, with additional predictors (QPC-X)

8. Quantile PC regression with time-varying parameters, with additional predictors (TVP-QPC-X)

All the models above, other than the AR(2) which is based on least squares, are estimated using the same default, automatic horseshoe prior we specified in the previous two sections. Whenever we consider models with exogenous predictors, we only estimate each class of models with one predictor at a time. Even though the horseshoe prior can accommodate ultra-high dimensional models, we are particularly interested in understanding the role of individual variables for forecasting inflation risks. For that reason, we do not consider here forecasting using the full model (all predictors), or principal components from the predictors, or forecast combinations. These are all reliable methods for improving forecast accuracy in any class of models, but they do not allow us to pin down the informational content of each individual predictor. Given these considerations, overall, 160 models are estimated, eight of which are models with no predictors and 152 of which are models with one individual financial indicator as an exogenous predictor.

Using data from 1990Q1 to 2019Q4, each model is estimated on the basis of the first half of the sample and used to produce four-quarters ahead and twelve-quarters ahead forecasts for 19 quantiles ($\tau = 0.05, 0.10, ..., 0.90, 0.95$), and thereafter forecasting follows a recursive scheme. We concentrate on the relative quantile scores at the first and last quantiles, that is the 5th and the 95th percentiles, to assess the ability of these models and indicators to predict low and high tail risks to inflation. The empirical analysis considers the quantile score of each competing model relative to the benchmark AR(2) model, by taking an average of such scores across all the forecasting periods. For each competing model j, the average (over the evaluation sample) quantile score for each τ and h is defined as:

$$QS_h^j(\tau) = \frac{1}{R_h}\sum_{t=1}^{R_h}[\pi_{t+h} - \hat{Q}_\tau(\pi_{t+h}|\boldsymbol{x}_t)][\mathbb{I}\{\pi_{t+h} \leq \hat{Q}_\tau(\pi_{t+h}|\boldsymbol{x}_t)\}], \tag{32}$$

where R_h is the length of the forecast evaluation sample (which depends on the forecast horizon, i.e. it is shorter for longer horizons). Smaller values of this loss function indicate better performance. We also use the predictive likelihood as a measure of general performance of the whole predictive density from each model we estimate (Korobilis, 2017). The predictive likelihood (PL) is obtained as the h-step ahead predictive density evaluated at the h-step ahead out-of-sample realisation of inflation. For the case of the PL, higher values indicate better performance.

4.3 Best performing models

When looking at the forecasting performance of the specific models, it appears that a number of credit and money volume indicators are particularly useful in predicting tail risks of core HICP inflation, outperforming several other financial indicators, especially in the context of quantile regression models featuring time-varying parameters.

For example, looking at forecasts for inflation tail risks four-quarters ahead (see upper panel in Table 2) a number of specific models appear to be very useful especially for forecasting the upper quantile ($\tau = 0.95$). This is the case, in particular, of quantile regressions with time-varying parameters (TVP-QAR-X) featuring bank loans to the private sector and total credit to the private sector, which lead to forecast gains very close to the best performing model, that is the PC model with time-varying parameters and stochastic volatility (TVP-PC-SV-X) featuring bank loans to firms (see results under QScore95). For the lowest quantile ($\tau = 0.05$) the improvement is more limited but non-negligible, especially for PC models with time-varying parameters and stochastic volatility (TVP-PC-SV-X) augmented with private sector loans, as well as for quantile regressions with time-varying parameters (TVP-QAR-X) featuring the M1 to GDP ratio or house prices (see results under QScore5). The overall density seems to be improved especially for quantile regressions with time-varying parameters (TVP-QAR-X) featuring the M1 to GDP ratio or loans to the private sector (see results under PL).

Also twelve-quarters ahead inflation tail risk forecasts can be improved, especially for upper tail risks ($\tau = 0.95$), by considering quantile regression-based PC models with time-varying parameters (TVP-QPC-X) featuring loans to households (see lower panel in Table 2). The latter specific model also appears to lead to the strongest improvement for the overall density (see results under PL). By contrast, gains for the lowest quantile ($\tau = 0.05$) are more limited but can still be detected especially for quantile regressions with time-varying parameters (TVP-QAR-X) featuring the ratio of private sector loans to GDP or the ratio to private sector total credit to GDP.

Overall, when assessing specific models, financial volume indicators such as loans to the private sector, loans to firms, loans to households, total credit to the private sector and the ratio of M1 to GDP often provide the largest forecasting gains, especially in the context of quantile regressions with time-varying parameters (TVP-QAR-X) or quantile regression-based Phillips curve models with time-varying parameters (TVP-QPC-X).

Table 2: *Best financial indicators and models for the prediction of core HICP inflation tail risks*

Measure	Ranking	Indicator	Specification	Score
		4-QUARTERS AHEAD		
QScore5	1st	loans to private sector	TVP-PC-SV-X	0.891
	2nd	M1/GDP	TVP-QAR-X	0.900
	3rd	house prices	TVP-QAR-X	0.900
QScore95	1st	loans to firms	TVP-PC-SV-X	0.761
	2nd	loans to private sector	TVP-QAR-X	0.767
	3rd	credit to private sector	TVP-QAR-X	0.780
PL	1st	M1/GDP	TVP-QAR-X	1.474
	2nd	loans to private sector	TVP-QAR-X	1.429
	3rd	house prices	QAR-X	1.383
		12-QUARTERS AHEAD		
QScore5	1st	private sector loans/GDP	TVP-QAR-X	0.951
	2nd	private sector credit/GDP	TVP-QAR-X	0.962
	3rd	yield curve	TVP-QAR-X	0.963
QScore95	1st	loans to households	TVP-QPC-X	0.635
	2nd	private sector credit/GDP	QAR-X	0.685
	3rd	loans to households/GDP	QAR-X	0.692
PL	1st	loans to households	TVP-QPC-X	1.552
	2nd	loans to households	QAR-X	1.336
	3rd	loans to households/GDP	QAR-X	1.295

Notes: PC stands for Phillips curve, QAR for quantile autoregression with two lags, AR for mean autoregression with two lags, TVP for time-varying parameters and SV for stochastic volatility. Low inflation tail risks are captured by the 5th percentile ($\tau = 0.05$) while high inflation tail risks are captured by the 95th percentile ($\tau = 0.95$). The lower blocks for each horizon reports the Predictive Likelihood (PL) which provides an evaluation of the forecast of the whole distribution of inflation. The last column reports the ratios of the predictive quantile score of the models described in each row to that of the AR(2) model. For the quantile scores, a value below 1 signals an improvement of the forecast relative to the benchmark and the lower the value the larger is the improvement. For the PL, any value above 1 signals an improvement of the forecast relative to the benchmark model and the higher the value of such ratio the larger the improvement.

4.4 The role of financial indicators

In order to understand what role the inclusion of financial indicators might play, it can be interesting to compare the evolution over time of the upper and lower quantile scores, as a measure of tail risk forecast errors, for different models. By comparing the evolution

of the quantile scores of the best models for the upper and lower quantiles ($\tau = 0.05$ and $\tau = 0.95$) among the quantile regression models with time-varying parameters - which are often among the best and which are the main focus of the paper - as highlighted in Table 2, with those of a similar model without the financial indicator we can derive some indication on the importance of considering such additional indicator when forecasting inflation tail risks. A similar comparison with the quantile scores of the same models with constant parameters, but all else equal, can give an idea on the importance of this specific modelling choice.

Starting with the best TVP-QAR model for the prediction of four-quarters ahead inflation low quantiles ($\tau = 0.05$), that is the TVP-QAR-X model featuring the M1 to GDP ratio, and comparing its quantile score with that of the TVP-QAR model (i.e., without any financial indicator) we can notice that the latter model leads to additional large forecast errors especially during the global financial crisis, that is around 2008 and 2009 (see left-hand side chart of the top panel of Figure 2). Similarly, the model with constant parameters (QAR-X) for M1 to GDP produces additional large forecast errors not only in 2008 and 2009, though smaller than those of the TVP-QAR model, but also in 2013, 2016 and 2017, by contrast to the benchmark TVP-QAR-X model for M1 to GDP (see right-hand side chart of the top panel of Figure 2).

As regards the best TVP-QAR model for the prediction of the highest quantile ($\tau = 0.95$) for inflation four-quarters ahead, that is the TVP-QAR-X model featuring loans to the private sector, the same model without this financial indicator leads to higher forecasting errors both in prolonged periods, such as between 2007 and 2009, and in specific quarters, such as in mid-2011 and late 2014 (see left-hand side chart of the bottom panel of Figure 2). The same model with constant parameters implies much larger forecast errors especially between 2010 and 2011 and in late-2014, compared to the model with time-varying parameters (see right-hand side chart of the bottom panel of Figure 2).

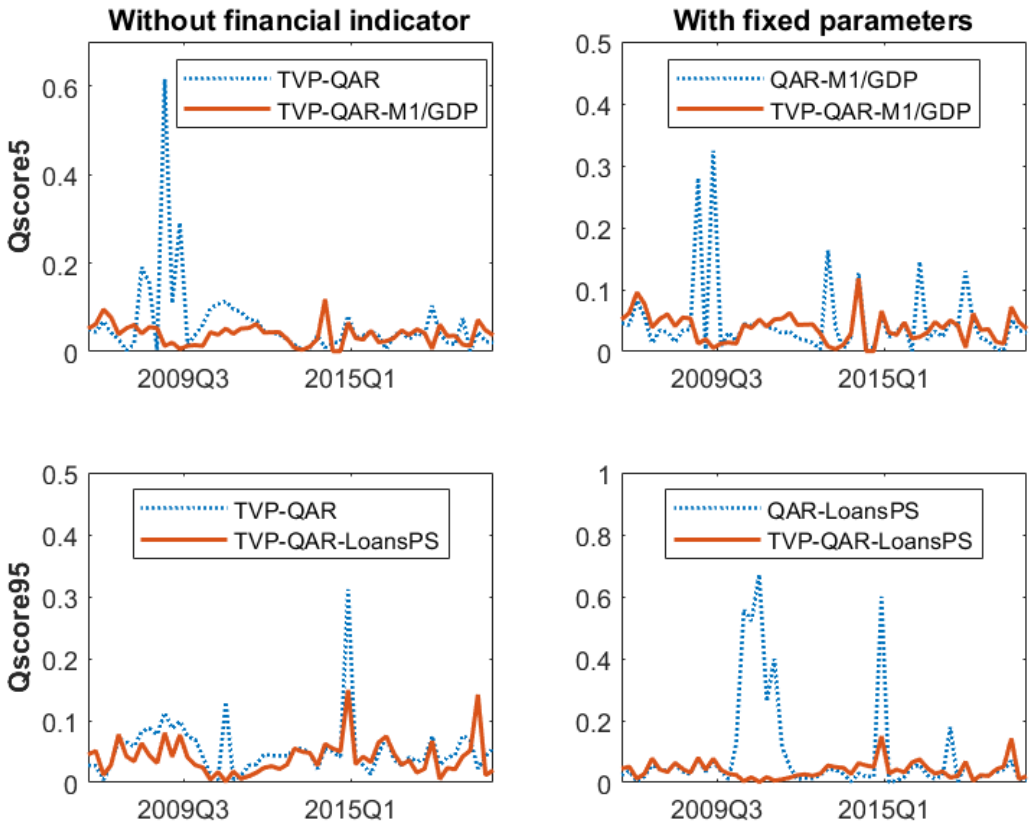

Figure 2: *Quantile score evolution for the best TVP-QAR-X model and alternative models: 4-quarter ahead*

A similar exercise with the best TVP-QAR model for the prediction of the lowest quantile ($\tau = 0.05$) of inflation twelve-quarters ahead, that is the TVP-QAR-X model featuring the ratio of loans to the private sector to GDP, suggests that the same model without this financial indicator leads to higher forecasting errors around 2009 and in mid-2016 (see left-hand side chart of the top panel of Figure 3). The same model with constant parameters implies much larger forecast errors especially around 2009, 2014 and 2016, compared to the model with time-varying parameters (see right-hand side chart of the top panel of Figure 3). As regards the upper quantile ($\tau = 0.95$), taking the time-varying parameters quantile regression PC augmented with loans to households as reference, the forecast error of the same model either without financial indicator or with fixed parameters are clearly higher for prolonged periods (bottom panel of Figure 3).

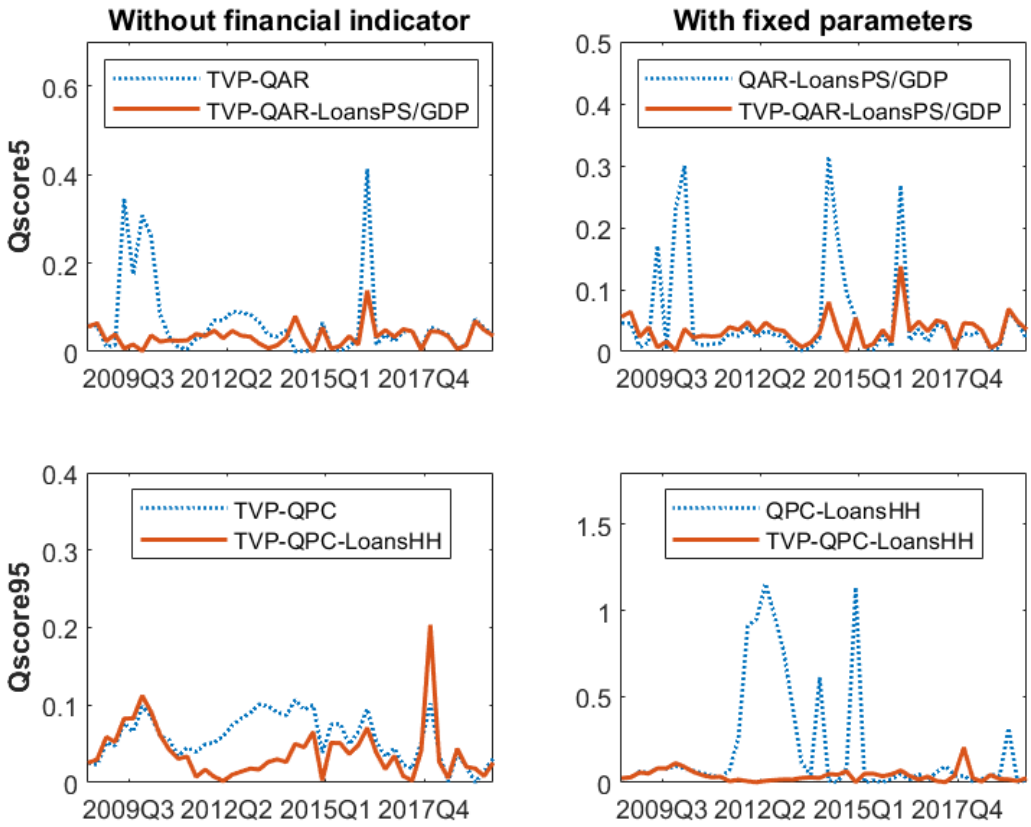

Figure 3: *Quantile score evolution for the best TVP-QAR-X and TVP-QPC-X models and alternative models: 12-quarter ahead*

Overall, for the prediction of tail risks of inflation both one-year and three-years ahead, it appears that the inclusion of the financial indicator outperforming other ones within TVP-QAR-X or TVP-QPC-X models explains a significant fraction of the reduction in forecasting errors compared to competing specific models. However, also the key modelling specification characterising such models, that is time-varying parameters, seems to be instrumental in explaining the good forecasting performance of the models highlighted.

The good forecasting properties of credit and money indicators for inflation tail risks appear consistent with economic intuition. Credit growth indicators, the coefficients of which tend to be positive within the estimated quantile regression models considered (see Figure C4 in Appendix C), can be seen as proxies of the degree of tightness of financial constraints for firms and households, which affect the price setting decisions of firms and the spending decisions of households. By contrast, the estimated coefficient for the ratio of M1 to GDP tends to be negative (see Figure C4 in Appendix C), which

could reflect the fact that increases in M1 in excess of GDP are likely to capture increased uncertainty which is typically associated with the postponement of expenditure thereby creating disinflationary pressures. From a theoretical perspective, these results appear to be consistent with the implications of the continuous-time monetary model of Brunnermeier and Sannikov (2016) allowing for endogenous risk dynamics, featuring heterogeneous agents and financial frictions. Within this model, credit and money volume aggregates emerge as particularly informative indicators, both in normal times and during financial crises. In normal times, credit and money quantitative aggregates can signal vulnerabilities before they appear in spreads and risk premia, while during financial crises they can provide valuable information on sectoral bottlenecks in the economy in the form of impaired balance sheets and debt overhang problems (see also the discussion in Brunnermeier and Sannikov (2014)).

5 Conclusion

We develop a methodology for modelling and forecasting inflation risks flexibly via time-varying parameter quantile regressions. A key methodological contribution is represented by a new Gibbs sampler for time-varying parameters that is highly efficient and can be easily adapted to other settings that admit familiar state-space forms and are notoriously computationally intensive, such as dynamic factor models and time-varying parameter VARs. In terms of forecasting accuracy, we show that our feasible TVP-QAR model indeed provides improvements over its constant parameter alternative, as well as traditional TVP regressions with stochastic volatility.

An application of this methodology to the prediction of euro area core inflation tail risks, with data spanning the past thirty years, points to a very good forecasting performance of quantile regressions with time-varying parameters augmented with specific credit and money-based indicators, both in the short and the medium run.

Follow-up work will concentrate on assessing the ability of the proposed modelling framework to enhance the prediction of the tail risks of other core macroeconomic and financial variables, such as real GDP and asset prices, both in the euro area and in other countries.

References

Adrian, T., N. Boyarchenko, and D. Giannone (2019): "Vulnerable Growth," *American Economic Review*, 109, 1263–89.

Amir-Ahmadi, P., C. Matthes, and M.-C. Wang (2020): "Choosing Prior Hyperparameters: With Applications to Time-Varying Parameter Models," *Journal of Business & Economic Statistics*, 38, 124–136.

Bhadra, A., J. Datta, Y. Li, and N. Polson (2020): "Horseshoe Regularisation for Machine Learning in Complex and Deep Models1," *International Statistical Review*, 88, 302–320.

Bhattacharya, A., A. Chakraborty, and B. K. Mallick (2016): "Fast sampling with Gaussian scale mixture priors in high-dimensional regression," *Biometrika*, 103, 985–991.

Brownlees, C. and A. B. Souza (2021): "Backtesting global Growth-at-Risk," *Journal of Monetary Economics*, 118, 312–330.

Brunnermeier, M. and Y. Sannikov (2016): "The I Theory of Money," Tech. Rep. w22533, National Bureau of Economic Research, Cambridge, MA.

Brunnermeier, M. K. and Y. Sannikov (2014): "Monetary Analysis: Price and Financial Stability," Tech. rep., ECB Forum on Central Banking, Sintra, Portugal.

Cai, Z. and X. Xu (2009): "Nonparametric Quantile Estimations for Dynamic Smooth Coefficient Models," *Journal of the American Statistical Association*, 104, 371–383.

Carriero, A., T. E. Clark, and M. Marcellino (2020): "Nowcasting Tail Risks to Economic Activity with Many Indicators," Working Paper No. 20-13, Federal Reserve Bank of Cleveland.

Carvalho, C. M., N. G. Polson, and J. G. Scott (2010): "The Horseshoe Estimator for Sparse Signals," *Biometrika*, 97, 465–480.

Chan, J. and I. Jeliazkov (2009): "Efficient simulation and integrated likelihood estimation in state space models," *International Journal of Mathematical Modelling and Numerical Optimisation*, 1, 101–120.

Chan, J. C. (2013): "Moving average stochastic volatility models with application to inflation forecast," *Journal of Econometrics*, 176, 162–172.

Cooley, T. F. and E. C. Prescott (1976): "Estimation in the Presence of Stochastic Parameter Variation," *Econometrica*, 44, 167–184.

Faust, J. and J. H. Wright (2013): "Forecasting Inflation," in *Handbook of Forecasting*, Elsevier, vol. 2, chap. 1, 2–56.

Gerlach, R. H., C. W. S. Chen, and N. Y. C. Chan (2011): "Bayesian Time-Varying Quantile Forecasting for Value-at-Risk in Financial Markets," *Journal of Business & Economic Statistics*, 29, 481–492.

Ghosh, P., X. Tang, M. Ghosh, and A. Chakrabarti (2016): "Asymptotic Properties of Bayes Risk of a General Class of Shrinkage Priors in Multiple Hypothesis Testing Under Sparsity," *Bayesian Analysis*, 11, 753–796.

Gonçalves, K. C. M., H. S. Migon, and L. S. Bastos (2020): "Dynamic Quantile Linear Models: A Bayesian Approach," *Bayesian Analysis*, 15, 335–362.

Griffin, J. E. and G. Mitrodima (2020): "A Bayesian Quantile Time Series Model for Asset Returns," *Journal of Business & Economic Statistics*, 0, 1–12.

Johnson, N. L., S. Kotz, and N. Balakrishnan (1994): *Continuous univariate distributions. Vol. 1.*, New York: Wiley & Sons, 2nd ed.

Khare, K. and J. P. Hobert (2012): "Geometric ergodicity of the Gibbs sampler for Bayesian quantile regression," *Journal of Multivariate Analysis*, 112, 108–116.

Kim, M.-O. (2007): "Quantile regression with varying coefficients," *Annals of Statistics*, 35, 92–108.

Koenker, R. and G. Bassett (1978): "Regression Quantiles," *Econometrica*, 46, 33–50.

Koop, G. and D. Korobilis (2012): "Forecasting Inflation Using Dynamic Model Averaging," *International Economic Review*, 53, 867–886.

Korobilis, D. (2017): "Quantile regression forecasts of inflation under model uncertainty," *International Journal of Forecasting*, 33, 11–20.

——— (2021): "High-Dimensional Macroeconomic Forecasting Using Message Passing Algorithms," *Journal of Business & Economic Statistics*, 39, 493–504.

Kozumi, H. and G. Kobayashi (2011): "Gibbs sampling methods for Bayesian quantile regression," *Journal of Statistical Computation and Simulation*, 81, 1565–1578.

Lim, D., B. Park, D. Nott, X. Wang, and T. Choi (2020): "Sparse signal shrinkage and outlier detection in high-dimensional quantile regression with variational Bayes," *Statistics and Its Interface*, 13, 237–249.

López-Salido, J. D. and F. Loria (2019): "Inflation at Risk," Discussion Papers No. 14074, Center for Economic Policy Research.

Makalic, E. and D. F. Schmidt (2016): "A Simple Sampler for the Horseshoe Estimator," *IEEE Signal Processing Letters*, 23, 179–182.

Pfarrhofer, M. (2021): "Tail forecasts of inflation using time-varying parameter quantile regressions," Tech. Rep. 2103.03632, Arxiv.

Rodrigues, T. and Y. Fan (2017): "Regression Adjustment for Noncrossing Bayesian Quantile Regression," *Journal of Computational and Graphical Statistics*, 26, 275–284.

Rossi, B. (2020): "Forecasting in the Presence of Instabilities: How Do We Know Whether Models Predict Well and How to Improve Them," *Journal of Economic Literature, forthcoming*.

Rossi, B. and T. Sekhposyan (2019): "Alternative tests for correct specification of conditional predictive densities," *Journal of Econometrics*, 208, 638–657.

Stock, J. H. and M. W. Watson (2007): "Why Has U.S. Inflation Become Harder to Forecast?" *Journal of Money, Credit and Banking*, 39, 3–33.

Tagliabracci, A. (2020): "Asymmetry in the Conditional Distribution of Euro-area Inflation," *Temi di discussione 1270, Bank of Italy*.

van der Pas, S. L., B. J. K. Kleijn, and A. W. van der Vaart (2014): "The horseshoe estimator: Posterior concentration around nearly black vectors," *Electronic Journal of Statistics*, 8, 2585–2618.

Wu, W. and Z. Zhou (2017): "Nonparametric Inference for Time-Varying Coefficient Quantile Regression," *Journal of Business & Economic Statistics*, 35, 98–109.

Yu, K. (2017): "Bayesian Quantile Regression," *https://expertsinuncertainty.net*, accessed Nov. 08, 2020.

Yu, K. and R. A. Moyeed (2001): "Bayesian quantile regression," *Statistics & Probability Letters*, 54, 437 – 447.

Appendix

A Bayesian inference in the quantile regression model

A.1 Linear quantile regression setting

Following Yu and Moyeed (2001) the quantile regression model has a parametric representation

$$y_t = x_t\beta(\tau) + \sigma(\tau)\varepsilon_t, \tag{A.1}$$

where $\beta(\tau)$ and $\sigma(\tau)$ are the regression coefficients and the scale parameter, respectively, for each quantile level τ, and ε_t are i.i.d. from a joint Asymmetric Laplace density of the form $\prod_{t=1}^{T} \frac{\tau(1-\tau)}{\sigma(\tau)^2}\left[e^{(1-\tau)\frac{\varepsilon_t}{\sigma(\tau)^2}}\mathbb{I}(\varepsilon_t \leq 0) + e^{-\tau\frac{\varepsilon_t}{\sigma(\tau)^2}}\mathbb{I}(\varepsilon_t > 0)\right]$. We can write the Asymmetric Laplace distribution using the following mixture representation (cf Kozumi and Kobayashi, 2011)

$$y_t = x_t\beta(\tau) + \theta(\tau)z_t + \sigma(\tau)\kappa(\tau)\sqrt{z_t(\tau)}u_t, \qquad u_t \sim N(0,1), \tag{A.2}$$

where $\theta(\tau) = \frac{1-2\tau}{\tau(1-\tau)}$ and $\kappa(\tau)^2 = \frac{2}{\tau(1-\tau)}$ and $z_t(\tau) \sim exp(\sigma(\tau)^2)$. Under this mixture representation the density of y_t is of the form

$$\prod_{t=1}^{T} \frac{1}{\sqrt{2\pi z_t(\tau)\sigma(\tau)^2\kappa(\tau)^2}} \exp\left\{-\frac{(y_t - x_t\beta(\tau) - \theta(\tau)z_t(\tau))^2}{2z_t(\tau)\sigma(\tau)^2\kappa(\tau)^2}\right\} \exp\left\{-\frac{z_t(\tau)}{\sigma(\tau)^2}\right\}, \tag{A.3}$$

which conditionally on $z_t(\tau)$ is a Normal density, while marginalising (i.e. integrating) over the unknown $z_t(\tau)$ gives the desired Asymmetric Laplace density (see the Appendix of Khare and Hobert, 2012, for a proof).

Given priors of the form

$$\beta(\tau) \sim N(0, V(\tau)), \tag{A.4}$$
$$\sigma(\tau) \sim IG(\rho_1, \rho_2), \tag{A.5}$$
$$z_t(\tau) \sim exp(\sigma(\tau)), \tag{A.6}$$

for each $\tau = 0.05, 0.10, ..., 0.90, 0.95$ [1], we obtain conditional posteriors of the form

$$\beta(\tau)|\bullet \sim N\left(\left(x'Ux + V(\tau)^{-1}\right)^{-1} \times \left(x'U\left[y - \theta(\tau)z(\tau)\right]\right), \left(x'Ux + V(\tau)^{-1}\right)^{-1}\right), \quad \text{(A.7)}$$

$$\sigma(\tau)^2|\bullet \sim inv - Gamma\left(\rho_1 + \frac{3T}{2}, \rho_2 + \sum_{t=1}^{T}\frac{\left(y_t - x_t\beta(\tau) - \theta(\tau)z_t(\tau)\right)^2}{2z_t(\tau)\kappa(\tau)^2} + \sum_{t=1}^{T} z_t(\tau)\right) \quad \text{(A.8)}$$

$$z_t(\tau)|\bullet \sim IG\left(\frac{\sqrt{\theta(\tau)^2 + 2\kappa(\tau)^2}}{|y_t - x_t\beta(\tau)|}, \frac{\theta(\tau)^2 + 2\kappa(\tau)^2}{\sigma(\tau)^2\kappa(\tau)^2}\right), \quad \text{(A.9)}$$

where $x = [x_1', ..., x_T']'$, $x = [y_1, ..., y_T]'$, and U is a $T \times T$ diagonal covariance matrix with t-th element $(z_t(\tau)\sigma(\tau)^2\kappa(\tau)^2)^{-1}$. In Equation (A.9) IG denotes the Inverse Gaussian distribution.[2] Kozumi and Kobayashi (2011) derive a posterior for $z_t(\tau)$ as in Equation (A.9) that is Generalised Inverse Gaussian (GIG) with different hyperparameters. The expression in (A.9) is derived by noting the property that the $IG(\mu, \lambda)$ distribution is a $GIG(\lambda/\mu^2, \lambda, -1/2)$ distribution, see Johnson et al. (1994).

A.2 Dealing with high-dimensional settings

Before we proceed with the time-varying parameter (TVP) version of the previous sampling algorithm, we discuss how we deal with high-dimensional versions of the Bayesian quantile regression model (the TVP quantile regression is such a model). Our focus is both on fast and efficient computation, as well as automatic shrinkage of the vector of regression coefficients.

Unlike the regular regression model, notice that in the quantile regression shrinkage is imperative even in the case where the number of predictors, p, is much smaller relative to the number of time series observations, T, that is, even when $p \ll T$. This is because we need to estimate a p-dimensional vector $\beta(\tau)$ for each quantile level $\tau = 0.05, 0.10, ..., 0.90, 0.95$. While around the median nearby quantiles can help assist estimate the β's more accurately, estimation in more extreme quantiles will rely on only a small proportion of the sample. Therefore, even small or moderate values of p can induce large estimation error of unrestricted estimators.

We specify a hiearchical shrinkage prior for $\beta(\tau)$ and, in particular, we follow

[1] Note that each $\beta(\tau)$ has its own prior variance $V(\tau)$ for each quantile level τ, while $\sigma(\tau)$ depends on the same hyperparmeters ρ_1, ρ_2 for all τ. This is because it is trivial to be noninformative for the variance parameters $\sigma(\tau)$, while this is not the case for $\beta(\tau)$: as we detail in the next subsection we are interested in regularising this parameter for the sake of estimation accuracy, therefore, $V(\tau)$ will be estimated adaptively (i.e. for each $\tau = 0.05, 0.10, ..., 0.90, 0.95$).

[2] While the inverse of a Gamma variate is distributed inverse Gamma, and vice-versa, the same is not true for the Normal (Gaussian) and Inverse Gaussian distributions.

Bhattacharya et al. (2016) who adopt a horseshoe prior of the form

$$\begin{aligned}
\beta(\tau)_i|\lambda(\tau)^2, \psi_i(\tau)^2 &\sim N\left(0, \lambda(\tau)^2\psi_i(\tau)^2\right), && \text{(A.10)}\\
\lambda(\tau) &\sim Cauchy^{+}\left(0,1\right), && \text{(A.11)}\\
\psi_i(\tau) &\sim Cauchy^{+}\left(0,1\right), && \text{(A.12)}
\end{aligned}$$

for $i = 1, ..., p$ and $\tau = 0.05, 0.10, ..., 0.90, 0.95$. The conditional posteriors of λ, ψ_i can be obtained if we consider the formulation of the horseshoe prior adopted in Makalic and Schmidt (2016). These authors write the horseshoe prior using the equivalent hierarchical notation

$$\begin{aligned}
\beta(\tau)_i|\lambda(\tau)^2, \psi_i(\tau)^2 &\sim N(0, \lambda(\tau)^2\psi_i(\tau)^2), && \text{(A.13)}\\
\lambda(\tau)^2|\xi(\tau) &\sim inv-Gamma\left(1/2, 1/\xi(\tau)\right), && \text{(A.14)}\\
\xi(\tau) &\sim inv-Gamma\left(1/2, 1\right), && \text{(A.15)}\\
\psi_i(\tau)^2|\zeta_i(\tau) &\sim inv-Gamma\left(1/2, 1/\zeta_i(\tau)\right), && \text{(A.16)}\\
\zeta_i(\tau) &\sim inv-Gamma\left(1/2, 1\right). && \text{(A.17)}
\end{aligned}$$

Conditional posteriors under this prior formulation are trivial to derive and exact formulas can be found in Makalic and Schmidt (2016).

The next step in our analysis is to sample efficiently the large dimensional vector $\beta(\tau)$ using Equation (A.7), especially when $p \gg T$. We follow again Bhattacharya et al. (2016) who propose an efficient way to sample from the Normal distribution using the Woodbury matrix identity. Calculation of the posterior covariance matrix of $\beta(\tau)$ relies on inverting the $p \times p$ matrix $(x'Ux + V^{-1})$ which requires $\mathcal{O}(p^3)$ algorithmic operations. The same number of algorithmic operations are needed to obtain the Cholesky decomposition of the posterior covariance, which is essential in order to generate from the desired Normal posterior distribution. In high dimensions, that is when p gets large, both these operations become computationlly cumbersome. Bhattacharya et al. (2016) propose instead the following sampling scheme[3]:

[3]This algorithm only works when the prior covariance matrix is diagonal, which is the case with the Horseshoe prior and the vast majority of Bayesian prior specifications.

Algorithm for efficient sampling from (A.7)

Step 1 Sample $\eta \sim N(0, V(\tau))$ and $\delta \sim N(0, I_T)$
Step 2 Set $v = \widetilde{x}\eta + \delta$
Step 3 Set $w = (\widetilde{x}V\widetilde{x}' + I_T)^{-1}[y - \theta(\tau)z(\tau) - v]$
Step 4 Set $\beta(\tau) = \eta + V\widetilde{x}'w$

where $\widetilde{x} = xU^{-1/2}$ where $U^{-1/2}$ is a $T \times T$ diagonal matrix with elements $(\sqrt{z_t(\tau)}\sigma(\tau)\kappa(\tau))^{-1}$ on its main diagonal. Instead of generating from a p-variate Normal posterior distribution, the algorithm above involves generating from the p-variate Normal prior distribution, and a T-variate standard Normal. As long as the prior covariance matrix is diagonal, generating from $\eta \sim N(0, V)$ is computationally trivial. Similar arguments hold for $\delta \sim N(0, I_T)$. The remaining transformations in the algorithm result from the Woodbudy identity (see Bhattacharya et al., 2016, for a straightforward proof) and they can be extremely efficient. The worst case complexity of the algorithm is $\mathcal{O}(T^2p)$, which provides huge gains relative to inverting and taking the Cholesky factor of the $p \times p$ matrix $(x'Ux + V^{-1})$.

Since our algorithm for estimating the quantile regression model is written in MATLAB, further gains can be achieved by replacing for loops with vector operators. This is very relevant here, because the algorithm requires for each MCMC iteration to also iterate through Equations (A.7)-(A.9) for each quantile level τ. MATLAB allows to generate from matrix-variate versions of the required posterior distributions, such that all parameters can be generated at once $\forall\ \tau \in \{0.05, 0.10, ..., 0.90, 0.95\}$.

A.3 Bayesian inference in the quantile regression model with time-varying parameters

Following the previous sections, the Bayesian time-varying parameter quantile regression model can be written as

$$y_t = x_t\beta(\tau)_t + \varepsilon_t, \qquad \varepsilon_t \sim ALD(\sigma(\tau)^2), \tag{A.18}$$

$$\beta_t(\tau) = \beta_{t-1}(\tau) + v_t, \qquad v_t \sim N(0, V(\tau)) \tag{A.19}$$

subject to the initial condition $\beta_0(\tau) \sim N(0, V_0(\tau))$, where x_t is a $1 \times p$ vector of predictors, and $V(\tau)$ is a $p \times p$ covariance matrix. Given that the ALD distribution for ε_t admits a mixture of Normals representation, it is trivial to treat the system above as a linear, conditionally Gaussian state-space model. However, doing so would result in recursive

sampler that would be quite inefficient.

We first note that the t-th observation y_t can be solved for $\Delta\beta_t(\tau) = \beta_t(\tau) - \beta_{t-1}(\tau)$ as

$$\begin{aligned} y_t &= x_t\beta_t(\tau) + \varepsilon_t \\ &= x_t\Delta\beta_t(\tau) + x_t\beta_{t-1}(\tau) + \varepsilon_t \\ &= x_t\Delta\beta_t(\tau) + x_t\Delta\beta_{t-1}(\tau) + x_t\beta_{t-2}(\tau) + \varepsilon_t \\ &... \\ &= x_t\Delta\beta_t(\tau) + x_t\Delta\beta_{t-1}(\tau) + ... + x_t\Delta\beta_2(\tau) + x_t\beta_1(\tau) + \varepsilon_t \end{aligned} \tag{A.20}$$

which shows that the coefficients at time t, $\beta(\tau)_t$ is simply the cumulative sum of changes over the previous time periods. More intuition can be built if we stack for all observations t and rewrite Equations (A.18)-(A.19) in the form

$$\begin{bmatrix} y_1 \\ y_2 \\ ... \\ y_{T-1} \\ y_T \end{bmatrix} = \begin{bmatrix} x_1 & 0 & ... & 0 & 0 \\ x_2 & x_2 & ... & 0 & 0 \\ ... & ... & ... & ... & ... \\ x_{T-1} & x_{T-1} & ... & x_{T-1} & 0 \\ x_T & x_T & ... & x_{T-1} & x_T \end{bmatrix} \begin{bmatrix} \beta_1(\tau) \\ \Delta\beta_2(\tau) \\ ... \\ \Delta\beta_{T-1}(\tau) \\ \Delta\beta_T(\tau) \end{bmatrix} + \begin{bmatrix} \varepsilon_1 \\ \varepsilon_2 \\ ... \\ \varepsilon_{T-1} \\ \varepsilon_T \end{bmatrix} \tag{A.21}$$

$$\begin{bmatrix} \beta_1(\tau) \\ \Delta\beta_2(\tau) \\ ... \\ \Delta\beta_{T-1}(\tau) \\ \Delta\beta_T(\tau) \end{bmatrix} = \begin{bmatrix} v_1 \\ v_2 \\ ... \\ v_{T-1} \\ v_T \end{bmatrix} \tag{A.22}$$

or more compactly

$$y = \mathcal{X}\beta^{\Delta}(\tau) + \varepsilon, \tag{A.23}$$

$$\beta^{\Delta}(\tau) = v, \tag{A.24}$$

where $\beta^{\Delta} = [\Delta\beta_1(\tau)', \Delta\beta_2(\tau)', ..., \Delta\beta_T(\tau)]'$ and $\mathcal{X}$ is the block triangular matrix shown analytically above. The first equation is a static linear regression with parameters $\beta^{\Delta}(\tau)$. The main characteristic of this equation is that it represents a high-dimensional setting, since the lower-triangular matrix $\mathcal{X}$ has dimensions $T \times Tp$, i.e. more covariates than observations. The second equation is an identity and, instead of having the interpretation of a state equation, it can be seen as a standard Normal prior for the difference between

$\beta_t(\tau)$ and $\beta_{t-1}(\tau)$. This high-dimensional representation shows clearly why shrinkage in TVP models is imperative, and why choice of the state covariance matrix ($V(\tau)$ here) is of paramount importance; see the discussion in Amir-Ahmadi et al. (2020).

It is notable that this representation of the TVP regression is equivalent to a minor reparameterisation of the formulation and algorithm of Chan and Jeliazkov (2009). Using their methods, the time-varying parameter quantile regression would be written as

$$y = \mathsf{X}\beta(\tau) + \varepsilon, \tag{A.25}$$

$$\beta(\tau) = H^{-1}v, \tag{A.26}$$

where

$$H = \begin{bmatrix} I_p & 0 & ... & 0 & 0 \\ -I_p & I_p & \ddots & 0 & 0 \\ \ddots & \ddots & \ddots & \ddots & \vdots \\ 0 & 0 & -I_p & I_p & 0 \\ 0 & 0 & 0 & -I_p & I_p \end{bmatrix}, \qquad \mathsf{X} = \begin{bmatrix} x_1 & 0 & ... & 0 & 0 \\ 0 & x_2 & \ddots & 0 & 0 \\ \vdots & \ddots & \ddots & 0 & \vdots \\ 0 & ... & 0 & x_{T-1} & 0 \\ 0 & ... & 0 & 0 & x_T \end{bmatrix} \tag{A.27}$$

and $\beta = [\beta_1(\tau)', ..., \beta_T(\tau)']'$. Note that if we compare (A.25) with (A.23) it holds that:

$$\mathsf{X}\beta(\tau) = \mathsf{X}H^{-1}H\beta(\tau) = (\mathsf{X}H^{-1})(H\beta(\tau)) = \mathcal{X}\beta^{\Delta}(\tau). \tag{A.28}$$

Similarly, if we left-multiply both sides of (A.26) with H, we obtain (A.24), showing that our suggested specification is a simple rotation of Chan and Jeliazkov (2009) using matrix H that creates first differences of the coefficients $\beta(\tau)$ and turns the diagonal matrix X into a lower triangular matrix. Despite the similarities, the formulation we propose makes full use of the fast algorithm of Bhattacharya et al. (2016) because the prior distribution of $\beta^{\Delta}(\tau)$ is diagonal (i.e. easy to sample from), while the distribution of $\beta(\tau)$ is tridiagonal; see Chan and Jeliazkov (2009) for its exact form. Therefore, our proposed Gibbs sampler is faster than the one proposed by Chan and Jeliazkov (2009), especially in high-dimensions (large p) and in the case of the quantile regression model where we need to sample TVPs for each quantile level τ.

Replacing ε with its mixture of Normal representation of the previous subsection, and adding the Horseshoe prior on $V(\tau)$ we can write the full Bayesian TVP quantile

regression model using the following equations

$$
\begin{aligned}
y &= \mathcal{X}\beta^{\Delta}(\tau) + \theta(\tau)z(\tau) + (\widetilde{S})u, && \text{(A.29)}\\
\beta^{\Delta}(\tau) &\sim N(0, V(\tau)), && \text{(A.30)}\\
V_{i,i}(\tau) &= \sigma(\tau)^2\lambda(\tau)^2\psi_i(\tau)^2, \quad i = 1, ..., Tp,\\
\lambda(\tau) &\sim Cauchy^{+}(0, 1), && \text{(A.31)}\\
\psi_i(\tau) &\sim Cauchy^{+}(0, 1), && \text{(A.32)}\\
\sigma(\tau) &\sim IG(\rho_1, \rho_2), && \text{(A.33)}\\
z_t(\tau) &\sim exp(\sigma(\tau)), \quad t = 1, ..., T, && \text{(A.34)}
\end{aligned}
$$

where $\widetilde{S}$ is a $T \times T$ diagonal matrix with diagonal element $\sigma(\tau)\kappa(\tau)\sqrt{z_t(\tau)}$.

A.4 Noncrossing quantiles

All estimation algorithms for quantile regression models, including the one presented above, assume that the quantile curves are fitted independently from each other. If we write the quantile regression model using the generic form

$$y_t = \mathcal{Q}_\tau(y_t|x_t) + \varepsilon_t, \tag{A.35}$$

then each curve $\mathcal{Q}_\tau(y_t|x_t)$ is estimated independently for each $\tau = 0.05, 0.1, ..., 0.90, 0.95$. This independence means that there is no mechanism in place in order to guarantee that estimates $\widehat{\mathcal{Q}}_\tau(y_t|x_t)$ satisfy the very definition of a quantile, that is the fact that $\widehat{\mathcal{Q}}_{\tau_1}(y_t|x_t) < \widehat{\mathcal{Q}}_{\tau_2}(y_t|x_t)$ when $\tau_1 < \tau_2$. This condition is also known as "quantile noncrossing". Various algorithms have been proposed in the literature to deal with this issue. Most algorithms propose to post-process the estimated quantile functions using some smoothing procedure/function. Such post-processing can work well, however, inevitably, will introduce some bias in quantile estimates, therefore choice of an appropriate algorithm is essential.

Here we use the recently proposed algorithm of Rodrigues and Fan (2017) for Bayesian quantile regression. This algorithm involves to first use a consistent MCMC-based estimator to obtain quantile regression estimates (such as the one outlined above), and then use a Gaussian process regression to smooth out the quantile estimates. In order to achieve this, Rodrigues and Fan (2017) note that exactly because

adjacent quantiles are correlated, one can use the following auxiliary model

$$\mathcal{Q}_{\tau,\tau^\star}(y_t|x_t) = \begin{cases} x_t\beta(\tau^\star) + \frac{\sigma(\tau^\star)}{1-\tau^\star}\log\left(\frac{\tau}{\tau^\star}\right), & if \quad 0 \leq \tau \leq \tau^\star, \\ \\ x_t\beta(\tau^\star) - \frac{\sigma(\tau^\star)}{\tau^\star}\log\left(\frac{1-\tau}{1-\tau^\star}\right), & if \quad \tau^\star \leq \tau \leq 1, \end{cases} \tag{A.36}$$

where $\mathcal{Q}_{\tau,\tau^\star}(y_t|x_t)$ is the induced quantile, and $\tau, \tau^\star \in \{0.05, 0.10, ..., 0.90, 0.95\}$. When $\tau = \tau^\star$ then $\mathcal{Q}_{\tau,\tau^\star}(y_t|x_t) \equiv \mathcal{Q}_\tau(y_t|x_t)$, that is, the induced quantile is equivalent to the estimated quantile based on our model. However, for all other levels of $\tau^\star$ we obtain additional induced quantile values that provide information for the quantile curve at τ. The principle is that the closer $\tau^\star$ is to τ, the more information its quantile curve can provide for estimation of the quantile curve at τ.

Given that there are 19 values in the set $\tau, \tau^\star \in \{0.05, 0.10, ..., 0.90, 0.95\}$, in our application $\mathcal{Q}_{\tau,\tau^\star}(y_t|x_t)$ is a 19×19 matrix. The diagonal elements of this matrix are identical to $\mathcal{Q}_\tau(y_t|x_t)$. Rodrigues and Fan (2017) specify a Gaussian process regression that ends up being equivalent to a weighting scheme where for each τ the quantiles $\mathcal{Q}_{\tau,\tau^\star}(y_t|x_t)$ take increasingly more weight the closer $\tau^\star$ is to τ. That way, the induced quantile at $\tau = \tau^\star$ (i.e. $\mathcal{Q}_\tau(y_t|x_t)$) takes the most weight and very distant quantiles get decreasing weights. It is very trivial to specify and implement this weighting/smoothing scheme, and we refer the reader to Rodrigues and Fan (2017) for more details.[4] Proposition 2 in that paper shows that this smoothed estimate of the quantiles is consistent, and a Monte Carlo study supports the good properties of this method.

[4] Their method introduces two new parameters, σ_κ^2 and b (using their notation). We follow the authors and set $\sigma_\kappa^2 = 100$ and we select the minimum b that provides a non-crossing solution.

B Data

B.1 Details on data definitions, derivations and sources

Table B1: List of euro area indicators

VARIABLE	FULL DESCRIPTION	UNIT	CATEGORY
Core HICP	HICP - All-items excluding energy and food	index	main variable of interest
Inflation expectations	Long-term inflation expectations	percent	Phillips curve determinant
Output gap	Output gap	percentage points	Phillips curve determinant
Import prices	Relative import prices	index	Phillips curve determinant
M1	M1	index	financial indicator: money
M1/GDP	M1 to GDP ratio	percent	financial indicator: money
M3	M3	index	financial indicator: money
M3/GDP	M3 to GDP ratio	percent	financial indicator: money
CreditPS	Credit to the private sector	index	financial indicator: credit
CreditPS/GDP	Credit to the private sector to GDP ratio	percent	financial indicator: credit
LoansPS	Bank loans to the private sector	index	financial indicator: credit
LoansPS/GDP	Bank loans to the private sector to GDP ratio	percent	financial indicator: credit
Loans to NFCs	Bank loans to non-financial corporations	index	financial indicator: credit
LoansNFC/GDP	Bank loans to non-financial corporations to GDP ratio	percent	financial indicator: credit
Loans to HHs	Bank loans to households	index	financial indicator: credit
LoansHH/GDP	Bank loans to households to GDP ratio	percent	financial indicator: credit
CorpBondSpr	Corporate bond spread	percentage points	financial indicator: spread
NFCLendingSpr	Firm lending rate spread	percentage points	financial indicator: spread
HHlendingSpr	Household lending rate spread	percentage points	financial indicator: spread
CISS	Composite Indicator of Systemic Stress	index	financial indicator: other
StockP	Dow Jones Euro Stoxx Price Index	index	financial indicator: other
HouseP	Residential property price index	index	financial indicator: other
Slope YC	Slope of the yield curve	percentage points	financial indicator: other

HICP - All-items excluding energy and food ("core HICP") ECB data from 1997 onwards (ECB Statistical Data Warehouse (SDW) code: ICP.M.U2.Y.XEF000.3.INX, quarterly averages) extended backwards to 1990 with Eurostat data (SDW code: ICP.M.U2.N.XEF000.4.INX, quarterly averages) and seasonally adjusted via Matlab X-13 Toolbox. Source: ECB and Eurostat.

Consensus Long-Term Inflation Expectations Consensus forecast, 6-10-years ahead, for the euro area from 2003 onwards (quarterly data from 2014Q2 onwards, extended back on the basis of semiannual data from April 2003 to October 2013, with quarterly missing data derived as averages of the two seminannual contiguous data), extended back to 1990Q1 with weighted average of country seminannual Consensus forecasts (for Germany, France, Itay, Spain and the Netherlands to

1995Q1 and for Germany, France and Itay to 1990Q1, with 2019 consumer spending weights at actual euro exchange rate and with quarterly missing data derived as averages of the two seminannual contiguous data). Source: Consensus Economics.

Output gap Principal component of three euro area output gap estimates (derived by interpolating annual estimates by EC, IMF and OECD). Source: European Commission, IMF, OECD and ECB calculations.

Relative import prices Difference between growth of deflator for imports of goods and services (Eurostat ESA2010 data, SDW code: MNA.Q.Y.I8.W1.S1.S1.C.P7._Z._Z._Z.IX.D.N from 1995Q1 onwards, extended backwards with AWM data: MTD from AWM19upd18) and core HICP growth (see above for details). Source: ECB and Eurostat.

M1 Index of notional stocks for M1 (SDW code: BSI.M.U2.Y.V.M10.X.I.U2.2300.Z01.E, end of quarter data). Source: ECB.

M1 to GDP ratio Ratio of M1 (index of notional stock, see above, rescaled to nominal stock values on the basis of outstanding amounts, SDW code: BSI.M.U2.Y.V.M10.X.1.U2.2300.Z01.E, with base December 2010) to nominal GDP (Eurostat ESA2010 data, SDW code: MNA.Q.Y.I8.W2.S1.S1.B.B1GQ._Z._Z._Z.eur.V._Z from 1995Q1 onwards, extended backwards with AWM data: YER*YED from AWM19upd18, quarterly data annualised). Source: ECB.

M3 Index of notional stocks for M3 (SDW code: BSI.M.U2.Y.V.M30.X.I.U2.2300.Z01.E, end of quarter data). Source: ECB.

M3 to GDP ratio Ratio of M3 (index of notional stock, see above, rescaled to nominal stock values on the basis of outstanding amounts, SDW code: BSI.M.U2.Y.V.M30.X.1.U2.2300.Z01.E, with base December 2010) to nominal GDP (Eurostat ESA2010 data, SDW code: MNA.Q.Y.I8.W2.S1.S1.B.B1GQ._Z._Z._Z.eur.V._Z from 1995Q1 onwards, extended backwards with AWM data: YER*YED from AWM19upd18, quarterly data annualised). Source: ECB.

Credit to the non-financial private sector Euro area credit to private non-financial sector from all sectors at market value, domestic currency, adjusted for breaks,

from the BIS Long series on credit to the non-financial sector database (BIS code: Q:XM:P:A:M:XDC:A, see https://www.bis.org/statistics/totcredit/totcredit.xlsx) from 1999Q1 onwards, extended back with weighted average of country data from the same BIS database (for Germany, France, Itay, Spain, Belgium, Finland and Portugal with GDP weights). Source: BIS.

Credit to the non-financial private sector to GDP ratio Euro area credit to private non-financial sector from all sectors at market value, percentage of GDP, adjusted for breaks, from the BIS Long series on credit to the non-financial sector database (Q:XM:P:A:M:770:A, see https://www.bis.org/statistics/totcredit/totcredit.xlsx) from 1999Q1 onwards, extended back with weighted average of country data from the same BIS database (for Germany, France, Itay, Spain, Belgium, Finland and Portugal with GDP weights). Source: BIS.

Bank loans to the non-financial private sector Loans to the non-financial private sector (NFPS) granted by Monetary and Financial Institutions (MFIs), adjusted for loan sales, securitisation and cash pooling activities (notional stock index rescaled to outstanding amounts in Eur millions with base December 2010): sum of loans to non-financial corporations and loans to households (see below for details). Source: ECB.

Bank loans to the non-financial private sector to GDP ratio Loans to NFPS (see above for details) to nominal GDP (Eurostat ESA2010 data: MNA.Q.Y.I8.W2.S1.S1.B.B1GQ._Z._Z._Z.eur.V._Z from 1995Q1 onwards, extended backwards with AWM data: YER*YED from AWM19upd18, quarterly data annualised). Source: ECB and Eurostat.

Bank loans to non-financial corporations Loans to non-financial corporations (NFCs) granted by Monetary and Financial Institutions (MFIs), adjusted for loan sales, securitisation and cash pooling activities (notional stock index rescaled to outstanding amounts in Eur millions with base December 2010 (SDW code: BSI.M.U2.Y.U.A20T.A.I.U2.2240.Z01.E from 2003 onwards, end of quarter data, extended back on the basis of internal ECB estimates). For details on the adjustment see the explanatory notes: www.ecb.europa.eu/press/pr/stats/md/shared/pdf/explanatorynoteonadjustedloans.en.pdf. Source: ECB.

Bank loans to non-financial corporations to GDP ratio Loans to NFCs (see above for details) to nominal GDP (Eurostat ESA2010 data, SDW code:

MNA.Q.Y.I8.W2.S1.S1.B.B1GQ._Z._Z._Z.eur.V._Z from 1995Q1 onwards, extended backwards with AWM data: YER*YED from AWM19upd18, quarterly data annualised). Source: ECB and Eurostat.

Bank loans to households Loans to households and non-profit institutions serving households granted by Monetary and Financial Institutions (MFIs), adjusted for loan sales, securitisation and cash pooling activities (notional stock index rescaled to outstanding amounts in Eur millions with base December 2010, SDW code: BSI.M.U2.Y.U.A20T.A.I.U2.2250.Z01.E from 2003 onwards, end of quarter data, extended back on the basis of internal ECB estimates). For details on the adjustment see the explanatory notes: www.ecb.europa.eu/press/pr/stats/md/shared/pdf/explanatorynoteonadjustedloans.en.pdf. Source: ECB.

Bank loans to households to GDP ratio Loans to households (see above for details) to nominal GDP (Eurostat ESA2010 data, SDW code: MNA.Q.Y.I8.W2.S1.S1.B.B1GQ._Z._Z._Z.eur.V._Z from 1995Q1 onwards, extended backwards with AWM data: YER*YED from AWM19upd18, quarterly data annualised). Source: ECB and Eurostat.

Composite Indicator of Systemic Stress Composite Indicator of Systemic Stress (CISS): quarterly averages of daily data (SDW code: CISS.D.U2.Z0Z.4F.EC.SS_CI.IDX from 1999 onwards, extended backwards on the basis of internal ECB estimates). Source: ECB.

Dow Jones Euro Stoxx Price Index Dow Jones Euro Stoxx Price Index, historical close, average of observations through period (SDW code: FM.Q.U2.EUR.DS.EI.DJEURST.HSTA), seasonally adjusted via Matlab X-13 Toolbox. Source: ECB.

Residential property price index Residential property prices, transaction value, index, all dwelling types, new and existing (SDW code: RPP.Q.I8.N.TD.00.3.00), seasonally adjusted via Matlab X-13 Toolbox. Source: ECB.

Slope of the Yield Curve Euro area 10-year government benchmark bond yield (SDW code: FM.M.U2.EUR.4F.BB.U2_10Y.YLD, quarterly average of monthly data) minus 3-month Euribor (historical close, average of observations through period, SDW code: FM.M.U2.EUR.RT.MM.EURIBOR3MD_.HSTA, quarterly average of monthly data, from 1994 onwards, extended backwards with AWM data: STN from AWM19upd18). Source: ECB.

Corporate bond spread Corporate bond yield (investment grade, quarterly average of monthly data, internal ECB estimates, from 1999 onwards, extended backwards with a weighted average of corporate bond yields from Global Financial Database for Germany, France, Italy and Spain, with weights based on the outstanding amounts of debt securities issued by non-financial corporations, SDW code: SEC.M."COUNTRY".1100.F33000.N.1.Z01.E.Z, with DE, FR, IT and ES in place of "COUNTRY", with a correction of German debt securities data in December 2011 linked to a reclassification) minus 3-month Euribor (historical close, average of observations through period, SDW code: FM.M.U2.EUR.RT.MM. EURIBOR3MD_.HSTA, quarterly average of monthly data, from 1994 onwards, extended backwards with AWM data: STN from AWM19upd18). Source: ECB and Global Financial Database.

Firm lending rate spread Composite indicator of bank lending rates for loans granted to non-financial corporations (SDW code: MIR.M.U2.B.A2A.A.R.A.2240.EUR.N, quarterly average of monthy data, from 2000 onwards, extended backwards on the basis of internal ECB estimates) minus 3-month Euribor (historical close, average of observations through period, SDW code: FM.M.U2.EUR.RT.MM.EURIBOR3MD_.HSTA, quarterly average of monthly data, from 1994 onwards, extended backwards with AWM data: STN from AWM19upd18). Source: ECB.

Household lending rate spread Composite indicator of bank lending rates for loans granted to households (weighted average of lending rates for loans to households for house purchase, SDW code: MIR.M.U2.B.A2C.A.R.A.2250.EUR.N, and lending rates for consumer credit, SDW code: MIR.M.U2.B.A2B.A.R.A.2250.EUR.N, in both cases quarterly average of monthy data, from 2000 onwards, extended backwards on the basis of internal ECB estimates, with weights based on the outstanding amounts of loans to households for house purchase and consumer credit) minus 3-month Euribor (historical close, average of observations through period: FM.M.U2.EUR.RT.MM. EURIBOR3MD_.HSTA, quarterly average of monthly data, from 1994 onwards, extended backwards with AWM data: STN from AWM19upd18). Source: ECB.

B.2 Plots of data

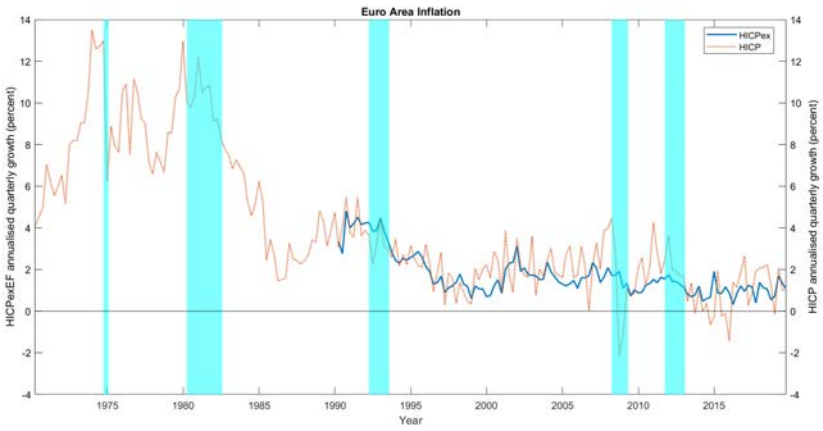

Figure B1: Euro area inflation

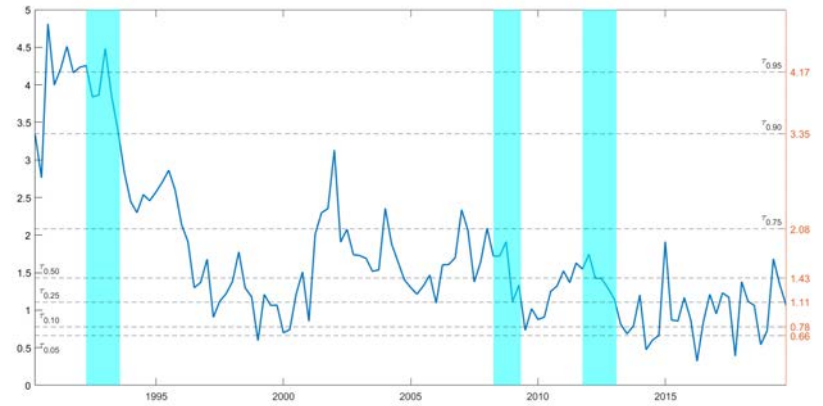

Figure B2: Euro area core inflation

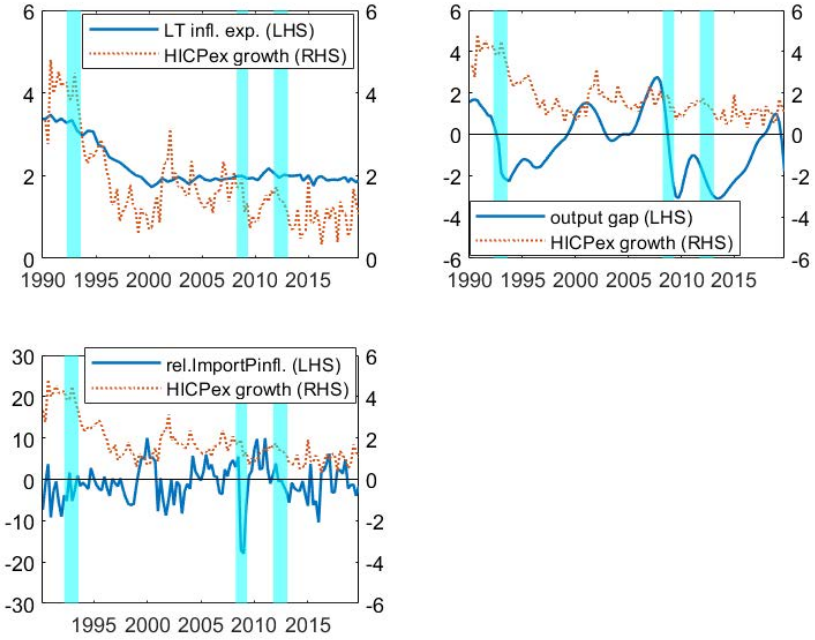

Figure B3: Determinants of Phillips curve

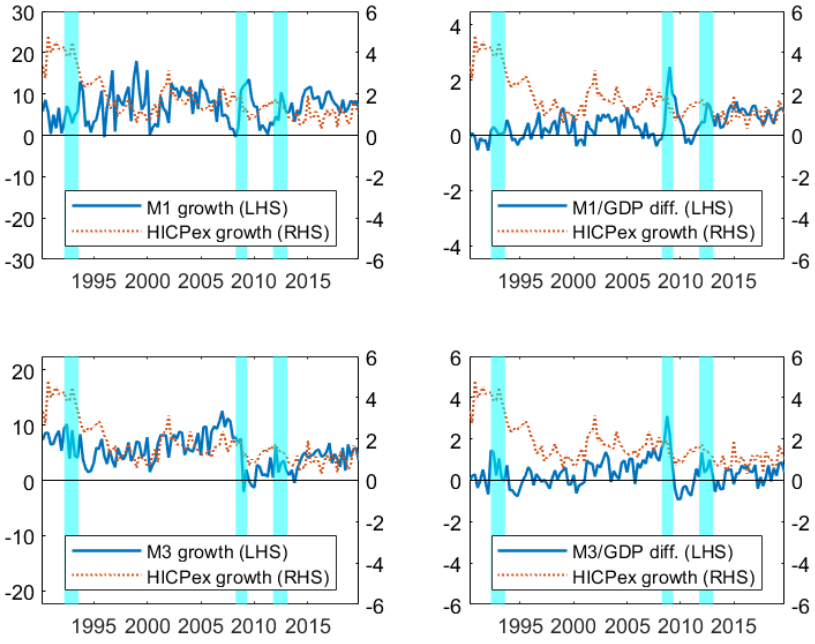

Figure B4: Financial indicators: money

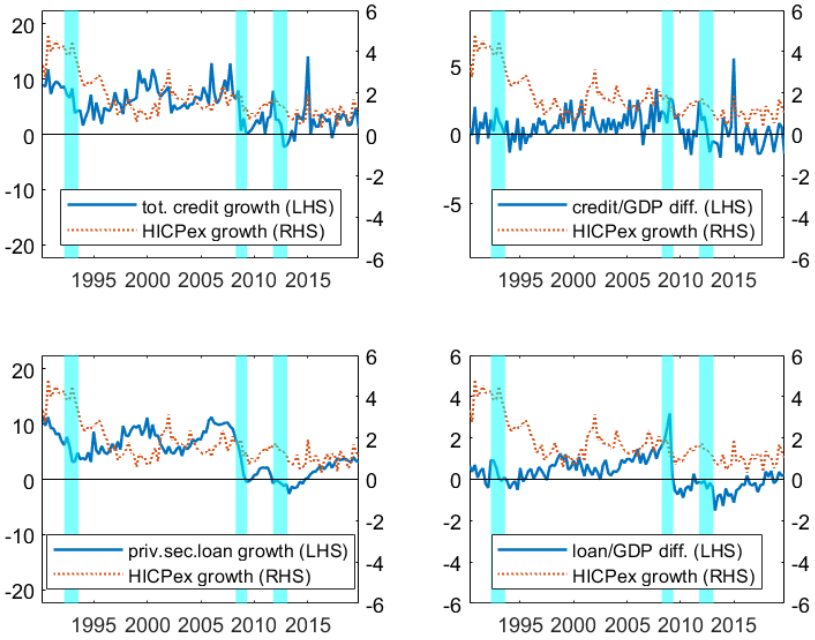

Figure B5: Financial indicators: credit

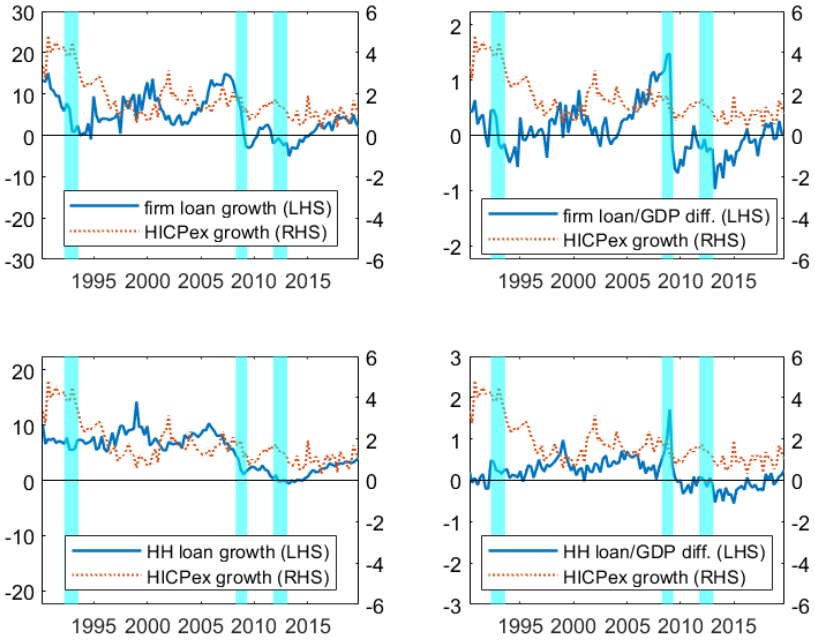

Figure B6: Financial indicators: sectoral bank loans

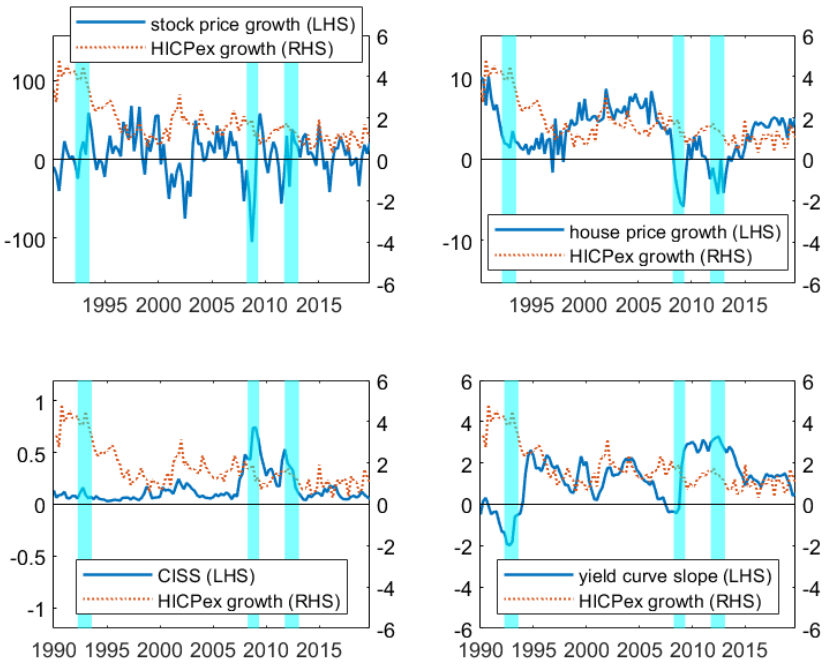

Figure B7: Financial indicators: asset prices, CISS and the yield curve

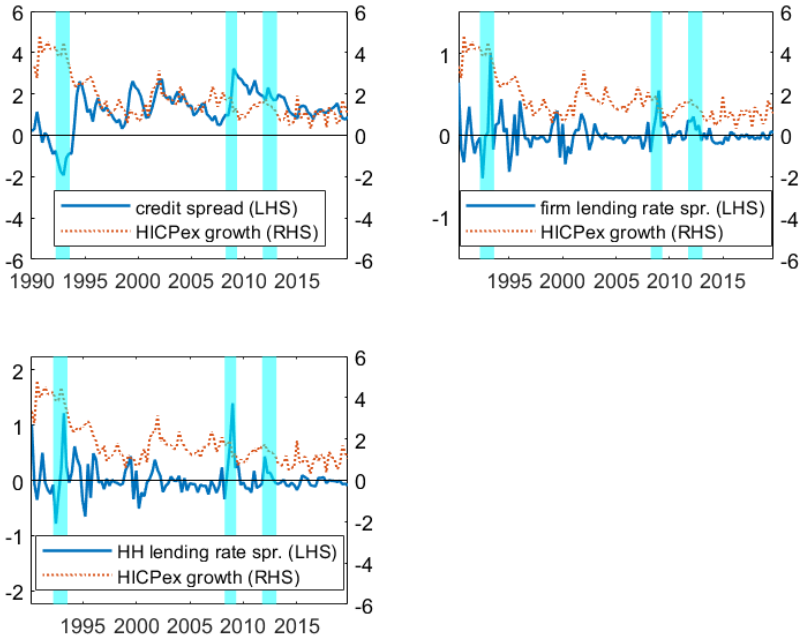

Figure B8: Financial indicators: spreads

B.3 Main properties of core inflation

Table B2: Main properties of euro area HICP excluding energy and food prices inflation

	Whole Sample 1990Q1-2019Q4	**Pre-Great Recession 1990Q1-2007Q4**	**Post-Great Recession 2008Q4-2019Q4**
		Summary Statistics	
Observations	119	71	48
Mean	1.8	2.2	1.1
Standard deviation	1.0	1.1	0.4
Minimum	0.3	0.6	0.3
Maximum	4.8	4.8	2.1
		Empirical Quantiles	
τ**=0.05**	0.66	0.88	0.50
τ**=0.10**	0.78	1.10	0.64
τ**=0.90**	3.35	4.00	1.72
τ**=0.95**	4.17	4.25	1.85
		Skewness and fat tails (Test Statistics)	
Skewness	4.988***	3.029***	0.145
Kurtosis	2.357***	0.247	1.004
Normality	0.695***	0.784***	0.644***

Notes: *** denotes statistical significance at 1% significance level

C Additional Results

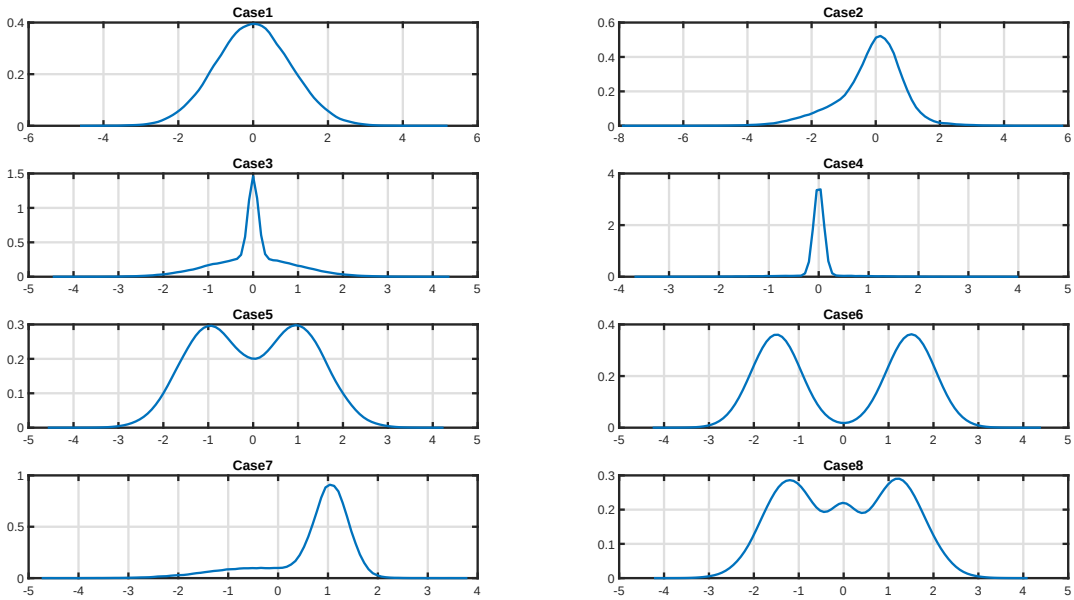

Figure C1: *Error distributions generated in the Monte Carlo study: 1) Normal, 2) Skewed, 3) Kurtotic, 4) Outlier, 5) Bimodal, 6) Bimodal, separate modes, 7) Skewed bimodal, and 8) Trimodal.*

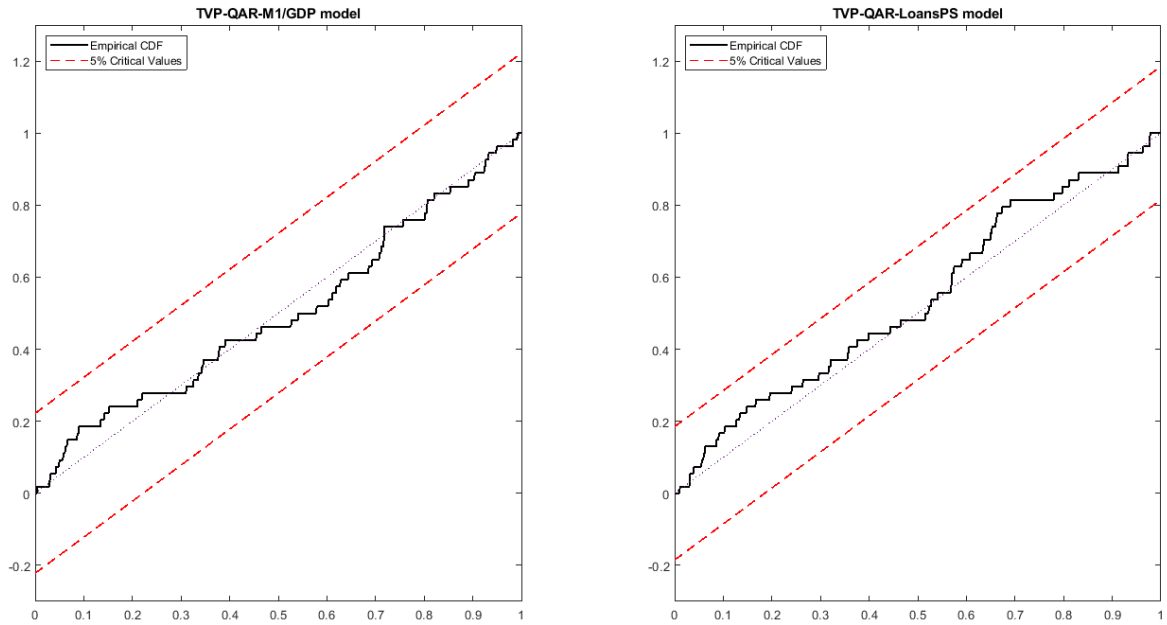

Figure C2: *Calibration tests of Rossi and Sekhposyan (2019) for the best models for 4-quarters ahead prediction*

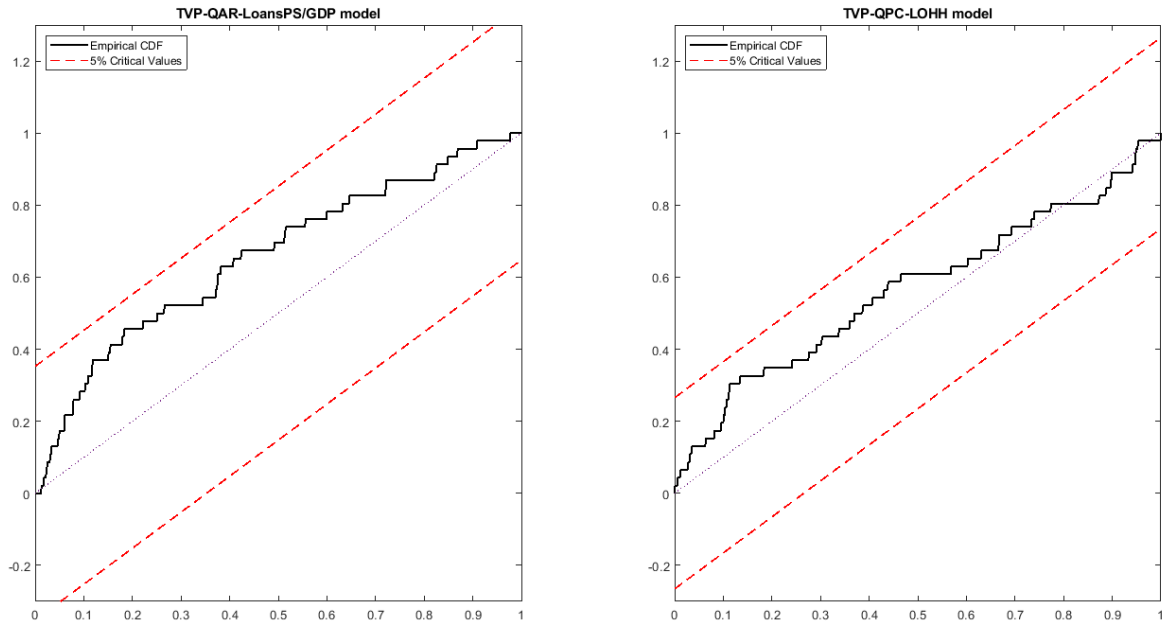

Figure C3: *Calibration tests of Rossi and Sekhposyan (2019) for the best models for 12-quarters ahead prediction*

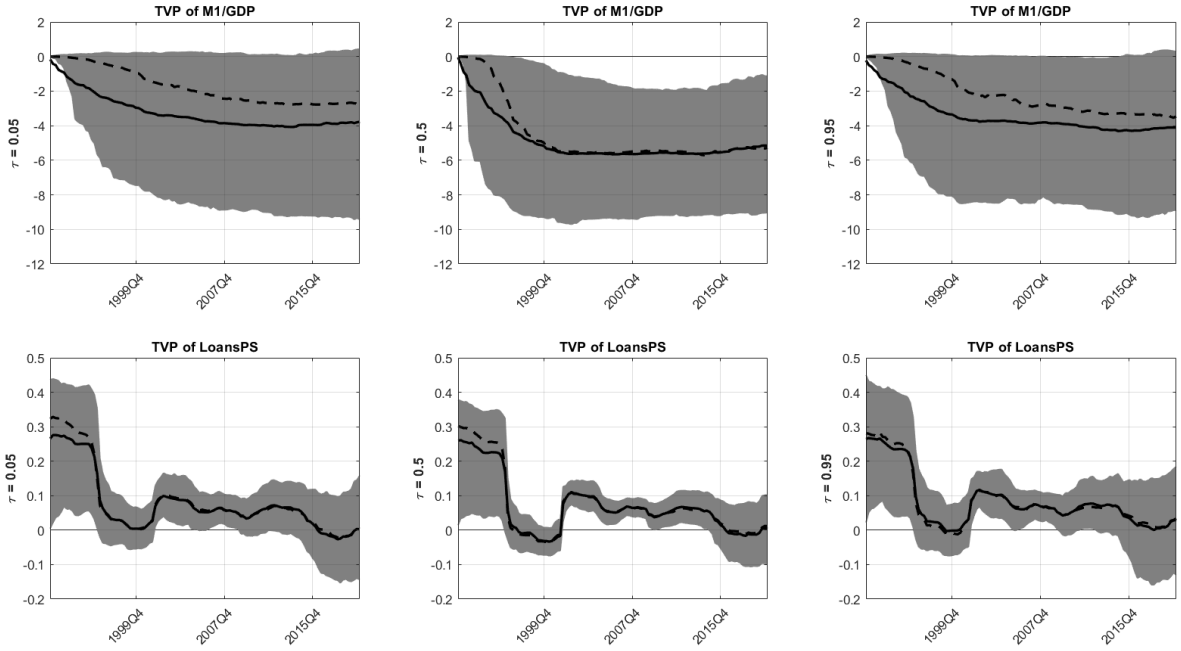

Figure C4: *Coefficient estimates for the financial indicator within the best TVP-QAR-X models for 4-quarters ahead prediction. The three panels at the top pertain to the coefficient corresponding to the ratio of M1 to GDP while the three panels at the bottom for loans to the private sector, for the quantiles* $\tau = [0.05, 0.5, 0.95]$. *Solid lines are the posterior means, dashed lines the posterior medians, while the shaded areas corresponds to the posterior* 16^{th} *and* 84^{th} *quantiles for each coefficient.*

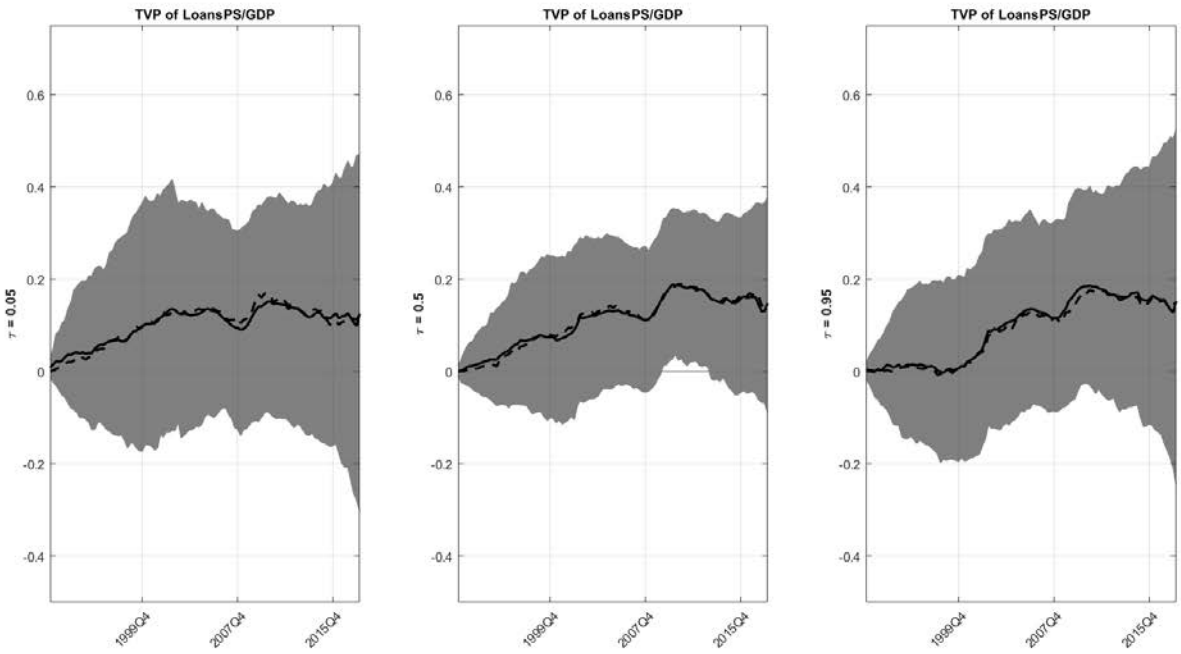

Figure C5: *Coefficient estimates for the financial indicator within the best TVP-QAR-X models for 12-quarters ahead prediction. The three panels pertain to the coefficient corresponding to the ratio of loans to the private sector to GDP, for the quantiles* $\tau = [0.05, 0.5, 0.95]$. *Solid lines are the posterior means, dashed lines the posterior medians, while the shaded areas corresponds to the posterior* 16^{th} *and* 84^{th} *quantiles for each coefficient.*

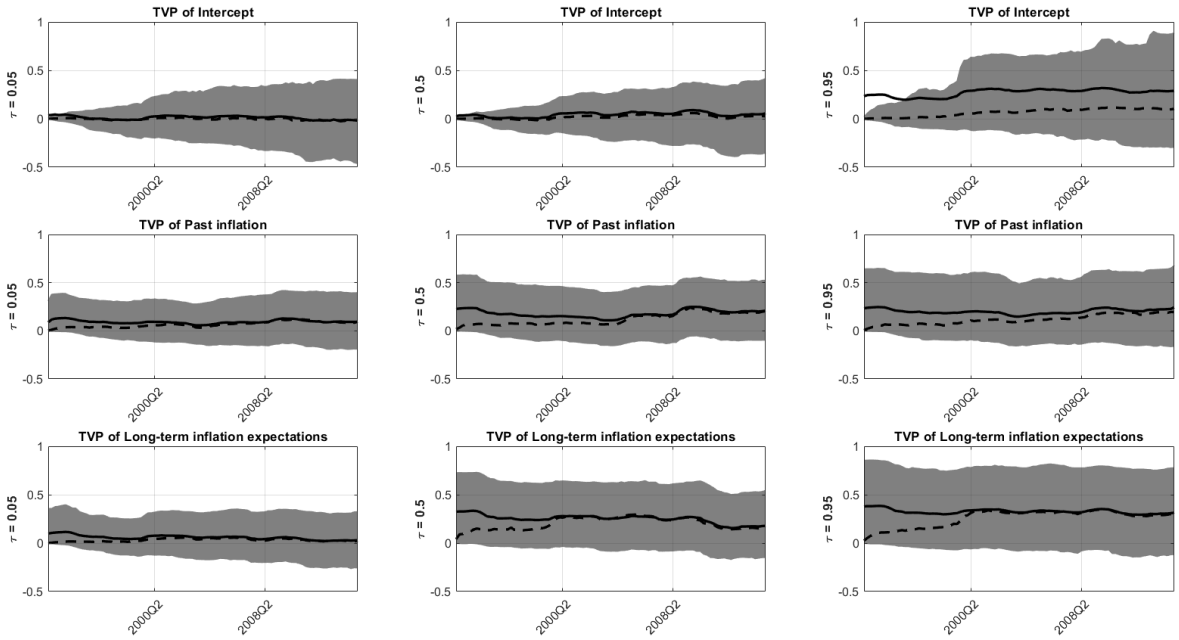

Figure C6: *Coefficient estimates for the all the regressors within the best TVP-QPC-X models for 12-quarters ahead prediction. The three panels at the top pertain to the coefficient corresponding to the intercept, the three panels in the middle to inflation inertia and the three panels at the bottom to long-term inflation expectations for the quantiles* $\tau = [0.05, 0.5, 0.95]$. *Solid lines are the posterior means, dashed lines the posterior medians, while the shaded areas corresponds to the posterior* 16^{th} *and* 84^{th} *quantiles for each coefficient.*

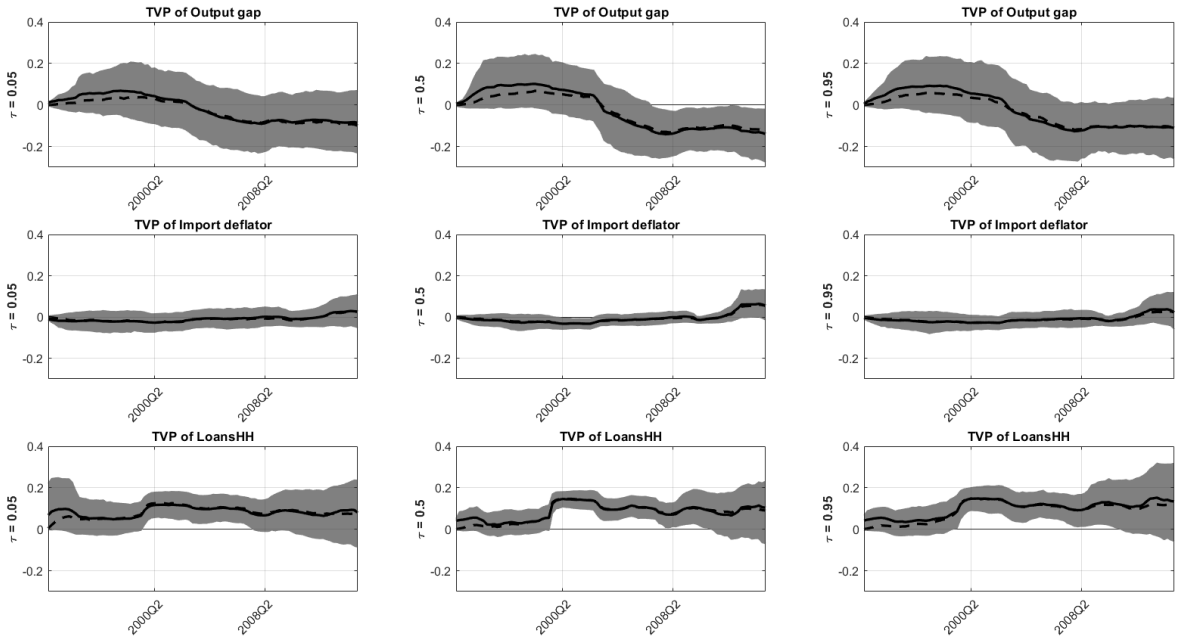

Figure C7: *Coefficient estimates for the all the regressors within the best TVP-QPC-X models for 12-quarters ahead prediction. The three panels at the top pertain to the coefficient corresponding to the output gap, the three panels in the middle to the change in relative prices and the three panels at the bottom to the financial indicator of loans to households, for the quantiles* $\tau = [0.05, 0.5, 0.95]$. *Solid lines are the posterior means, dashed lines the posterior medians, while the shaded areas corresponds to the posterior* 16^{th} *and* 84^{th} *quantiles for each coefficient.*

Acknowledgements

The opinions in this paper are those of the authors and do not necessarily reflect the views of the European Central Bank or the Eurosystem. We would like to thank Roberto Casarin, Todd Clark, Frank Diebold, Ana Galvao, Kostas Kalogeropoulos, Luca Rossini, Frank Schorfheide, participants at the 11th ECB Workshop on Forecasting Techniques and at the 2021 Annual Conference of the International Association for Applied Econometrics (IAAE), and participants in seminars at University of Pennsylvania, LSE joint Statistics/Economics seminars, and Ca'Foscari University Venice, for helpful discussions and comments.

Dimitris Korobilis
University of Glasgow, Glasgow, United Kingdom; email: dikorobilis@googlemail.com

Bettina Landau
European Central Bank, Frankfurt am Main, Germany; email: Bettina.Landau@ecb.europa.eu

Alberto Musso
European Central Bank, Frankfurt am Main, Germany; email: alberto.musso@ecb.europa.eu

Anthoulla Phella
European Central Bank, Frankfurt am Main, Germany; email: Anthoulla.Phella@ecb.europa.eu

Postal address 60640 Frankfurt am Main, Germany
Telephone +49 69 1344 0
Website www.ecb.europa.eu

PDF ISBN 978-92-899-4853-1 ISSN 1725-2806 doi:10.2866/861413 QB-AR-21-091-EN-N